Zoological Journal of the Linnean Society, 2018, **185**, 925–957. With 16 figures.

The phylogeny of Ryocalanoidea (Copepoda, Calanoida) based on morphology and a multi-gene analysis with a description of new ryocalanoidean species

JASMIN RENZ[1]*, ELENA L. MARKHASEVA[2] AND SILKE LAAKMANN[3,4]

[1]*German Centre for Marine Biodiversity Research (DZMB), Senckenberg am Meer, Martin-Luther-King Platz 3, 20146 Hamburg, Germany*
[2]*Laboratory of Marine Research, Zoological Institute, Russian Academy of Sciences, Universitetskaya nab. 1, 199034, St. Petersburg, Russia*
[3]*German Centre for Marine Biodiversity Research (DZMB), Senckenberg am Meer, Südstrand 44, 26382 Wilhelmshaven, Germany*
[4]*Helmholtz Institute for Functional Marine Biodiversity at the University of Oldenburg (HIFMB), Ammerländer Heerstraße 231, 26129 Oldenburg, Germany*

Received 24 November 2017; revised 1 August 2018; accepted for publication 2 September 2018

Two new species of ryocalanoid copepods (Crustacea: Calanoida), ***Ryocalanus squamatus* sp. nov.** and ***Yrocalanus kurilensis* sp. nov.** are described together with a female of *Ryocalanus infelix* Tanaka, 1956, type species for the genus *Ryocalanus* Tanaka, 1956, from abyssal depths in the Kurile-Kamchatka trench. The new species can be assigned to the superfamily Ryocalanoidea based on the segmentation and armature of the swimming legs and the modification of the male right antennule. A new interpretation of the fusions of segments in the male right antennule of *Ryocalanus* shows the marked differences between the ryocalanoidean genera. The status of Ryocalanoidea within the Calanoida is discussed based on morphology and a first molecular multi-gene analysis with cytochrome oxidase subunit I, cytochrome *b*, nuclear ribosomal 18S and 28S rDNA and internal transcribed spacer 2. This analysis supports the close interrelationship between Ryocalanoidea and Spinocalanoidea. The monophyletic status of Ryocalanoidea could not be retrieved in the phylogenetic analysis, as specimens of *Yrocalanus* formed a clade within Spinocalanoidea. The inconclusive results between morphological and molecular analyses are discussed with a proposition to keep the current system until more males of taxa belonging to the Spinocalanoidea are discovered, as the male antennule plays a crucial role in the interpretation of relationships between Ryocalanoidea and Spinocalanoidea.

ADDITIONAL KEYWORDS: Calanoida – *COI* – cytochrome *b* – 18S – 28S – ITS2 – molecular phylogeny – Ryocalanoidea – *Ryocalanus* – Spinocalanoidea – *Yrocalanus*.

INTRODUCTION

Within the order of Calanoida, the superfamilies Ryocalanoidea, Spinocalanoidea and Clausocalanoidea are considered to represent the evolutionarily most recently diverged lineages (Park, 1986), with the divergence of Spinocalanoidea and Clausocalanoidea hypothesized to be the most recent one (Blanco-Bercial *et al.*, 2011). The superfamily Ryocalanoidea was established by Andronov (1974), based on a single male of *Ryocalanus infelix* described by Tanaka (1956). Park (1986) recognized the family Spinocalanidae Vervoort, 1951, previously included in Clausocalanoidea by Andronov (1974), to form a separate superfamily Spinocalanoidea based on the fact that the mostly bathypelagic Spinocalanoidea have less specialized features such as the presence of an outer seta on the maxilla and the swimming leg setation (Park, 1986). Park also noted the similarity of mouthparts and swimming legs of Ryocalanoidea and Spinocalanoidea, but pointed out the marked difference between these taxa, based on the grasping right antennule of males.

Spinocalanoidea currently contain two families: Spinocalanidae and Arctokonstantinidae. The latter

*Corresponding author. E-mail: jrenz@senckenberg.de
[Version of Record, published online 27 November 2018; http://zoobank.org/urn:lsid:zoobank.org:pub:6F519A8-BB5F-4CCD-BE41-82D3F03E14BF]

family was established by Markhaseva & Kosobokova (2001) and later treated as a synonym for Spinocalanidae by Boxshall & Halsey (2004). Markhaseva (2008) and Markhaseva & Schulz (2008) gave a detailed analysis of Arctokonstantinidae, concluding that, based on the derived morphology of the oral parts, as well as the basis and endopod of the first leg, this family represents a monophyletic group. *Foxtonia* Hulsemann & Grice, 1963 and *Sognocalanus* Fosshagen, 1967, previously placed in Spinocalanidae and Bathypontiidae, were placed in Arctokonstantinidae (Markhaseva, 2008) together with *Arctokonstantinus* Markhaseva & Kosobokova, 2001, *Foxtosognus* Markhaseva, 2008 and *Caudacalanus* Markhaseva & Schulz, 2008.

In recent studies, genetic analyses of copepods have generated new insights into the origin and evolution of the Calanoida (e.g. Ohtsuka & Nishida, 2017). Both, mitochondrial and nuclear molecular markers have been used for phylogenetic analyses to elucidate the evolutionary history of living organisms and have been proven to be useful in reconstructing copepod phylogenetic relationships (e.g. Blanco-Bercial *et al.*, 2011; Laakmann *et al.*, 2012; Bradford-Grieve *et al.*, 2014, 2017). While species and population levels can be resolved based on mitochondrial gene fragments like cytochrome *c* oxidase subunit I (*COI*) (e.g. Bucklin *et al.*, 2003; Goetze, 2003; Eyun *et al.*, 2007; Aarbakke *et al.*, 2014; Questel *et al.*, 2016) and cytochrome *b* (Provan *et al.*, 2009; Milligan *et al.*, 2011), nuclear 18S rDNA, 28S rDNA and internal transcribed spacer 2 (ITS2) (e.g. Braga *et al.*, 1999; Bucklin *et al.*, 2003; Laakmann *et al.*, 2012) are more conserved and thus informative for phylogenetic analyses at intergeneric and higher taxonomic levels.

Multi-gene analyses of the calanoid superfamilies have been made to investigate the relationships within the Calanoida (Blanco-Bercial *et al.*, 2011; Bradford-Grieve *et al.*, 2014) by using both mitochondrial and nuclear ribosomal gene regions. These analyses demonstrated a high support of the morphology-based phylogeny by Andronov (1974) with its amendments made by Bowman & Abele (1982) and Park (1986). These molecular-based phylogenetic studies did not, however, include representatives of the superfamilies Ryocalanoidea and Epacteriscidae, and refinements in the currently available phylogeny are expected when new data are added.

The discovery of two new species of ryocalanid copepods in the Kurile-Kamchatka trench belonging to the genera *Ryocalanus* Tanaka, 1956 and *Yrocalanus* Renz, Markhaseva & Schulz, 2012 and the description of the previously unknown female of *Ryocalanus infelix*, the type species of the Ryocalanidae, presented an opportunity to combine morphological and molecular data to further our knowledge on the phylogeny of the Calanoida.

Our morphological studies were complemented with molecular analyses of ryocalanoidean and spinocalanoidean copepod species using multi-gene approaches to gain insight into the relationship between the evolutionarily youngest calanoid copepod families from a molecular perspective. The phylogeny of the Ryocalanoidea is discussed, based on a combined morphological and molecular approach.

MATERIAL AND METHODS

Copepods for morphological analysis were collected by RV *Sonne* (SO223) in the Kurile-Kamchatka trench and abyssal plain during the KuramBio expedition (Kurile-Kamchatka Biodiversity Study) in 2012. Sampling was carried out above the sea bed at depths of 4863–5400 m using a closing epibenthic sledge (Brandt & Barthel, 1995; Brenke, 2005) with a mesh size of 300 µm. Samples were fixed in either 96% pure ethanol or 4% buffered formalin.

Prior to dissection, specimens were cleared in lactic acid and some were stained by adding a solution of chlorazol black E dissolved in 70% ethanol/30% water. All figures were prepared using a *camera lucida* on a Zeiss Axioskop compound microscope fitted with interference contrast optics.

Free segments of the antennule are designated by Arabic numerals, ancestral segments by Roman numerals (Huys & Boxshall, 1991); one seta and one aesthetasc attached to a segment of the antennule are designated as: 1s + 1ae, while ? designates a visible scar for which it is not possible to identify the nature of the element.

The system of morphological nomenclature is based on that of Huys & Boxshall (1991). Type specimens are deposited at the Senckenberg Museum Frankfurt (SMF), Germany.

Molecular genetic analyses

Copepods for molecular analysis were collected by RV *Meteor* during the DIVA III expedition (Latitudinal Gradients in Biodiversity in the deep Atlantic) within the CeDAMar project (Census of the Diversity of Abyssal Marine Life) in 2009 and by RV *Sonne* (SO223) in the Kurile-Kamchatka trench and abyssal plain during the KuramBio expedition in 2012. Sampling was carried out as for morphological analysis and fixed in 96% pure ethanol.

Molecular genetic analyses were conducted on a total of 19 individuals with 11 ryocalanoidean, six spinocalanoidean and two clausocalanoidean specimens (Table 1). Genomic DNA was extracted from total specimens or parts of individuals using the QIAGEN DNeasy blood and tissue kit (QIAGEN) following the manufacturer's protocol with overnight lysis. PCR amplifications for five different gene fragments were

Table 1. Overview of individuals of calanoid copepods sampled for the molecular genetic analyses

ID	Species	Stage	Size [mm]	Sampling					Molecular Marker; GenBank Accession Numbers				
				Cruise	Region	Longitude/Latidude	Date	Depth [m]	18S	28S	ITS2	*COI*	*Cytb*
SPINOCALANOIDEA													
Spinocalanidae													
358	*Spinocalanus abyssalis*	female	–	DIVA 3	Atlantic	30.5228° N 28.5869° W	19.08.2009	1000–1500	MF796501	MF796482	–	MF796468	MF796440
360	*Spinocalanus cf. magnus*	female	2.40	DIVA 3	Atlantic	30.5228° N 28.5869° W	19.08.2009	1000–1500	MF796502	MF796483	MF796451	MF796469	–
361	*Spinocalanus aspinosus*	female	1.55	DIVA 3	Atlantic	30.5228° N 28.5869° W	19.08.2009	1000–1500	MF796503	MF796484	–	MF796470	MF796441
Arctokonstantinidae													
351	*Caudacalanus* sp. 2	female	–	Kurambio	Pacific	40.5808° N 151.0089° E	28.08.2012	5399	MF796504	MF796485	MF796452	MF796471	MF796442
352	*Caudacalanus* sp. 1	female	–	Kurambio	Pacific	40.5808° N 151.0089° E	28.08.2012	5399	MF796505	MF796486	MF796453	MF796472	MF796443
362	*Caudacalanus* sp. 3	female	–	DIVA 3	Atlantic	14.9919° S 29.9469° W	30.07.2009	5131	MF796506	MF796487	MF796454	MF796473	MF796444
RYOCALANOIDEA													
Ryocalanidae													
JR1	*Ryocalanus* sp. 5	female	8.70	DIVA 3	Atlantic	29.3233° N 28.6428° W	1.8.08.2009	4338	MF796507	MF796488	MF796455	MF796474	–
JR2	*Ryocalanus* sp. 7	female	5.70	DIVA 3	Atlantic	29.3233° N 28.6428° W	1.8.08.2009	4338	MF796508	MF796489	MF796456	MF796475	–
JR3	*Ryocalanus* sp. 1	CV♀	4.90	DIVA 3	Atlantic	29.3233° N 28.6428° W	1.8.08.2009	4338	MF796509	MF796490	MF796457	MF796476	–
JR4	*Ryocalanus* sp. 1	CIV	4.00	DIVA 3	Atlantic	3.9636° S 28.0853° W	06.08.2009	5168	MF796510	MF796491	MF796458	–	–
JR5	*Ryocalanus brasilianus*	female	–	DIVA 3	Atlantic	26.5864° S 35.2219° W	22.07.2009	4484	MF796511	MF796492	MF796459	MF796477	MF796445
346	*Yrocalanus kurilensis* sp. nov.	male	1.55	Kurambio	Pacific	39.7217° N 147.1653° E	31.08.2012	5224	MF796512	MF796493	MF796460	–	–
347	*Yrocalanus kurilensis* sp. nov.	female	1.90	Kurambio	Pacific	42.2422° N 151.7189° E	20.08.2012	5125	MF796513	MF796494	MF796461	–	MF796446
348	*Ryocalanus infelix*	male	2.15	Kurambio	Pacific	43.5794° N 153.9703° E	17.08.2012	5376	MF796514	MF796495	MF796462	MF796478	MF796447
349	*Ryocalanus infelix*	female	2.65	Kurambio	Pacific	43.9764° N 157.3064° E	30.07.2012	5423	MF796515	MF796496	MF796463	MF796479	MF796448
350	*Yrocalanus kurilensis* sp. nov.	female	1.65	Kurambio	Pacific	46.2550° N 155.5508° E	23.08.2012	4830	MF796516	MF796497	MF796464	–	–
363	*Ryocalanus squamatus* sp. nov.	female	–	Kurambio	Pacific	42.2422° N 151.7189° E	20.08.2012	5125	MF796517	MF796498	MF796465	MF796480	MF796449
CLAUSOCALANOIDEA **(Outgroup taxa)**													
Aetideidae													
364	*Prolutamator hadalis*	female	–	DIVA 3	Atlantic	26.5864° S 35.2219° W	22.07.2009	4484	MF796518	MF796499	MF796466	MF796481	MF796450
Euchaetidae													
359	*Paraeuchaeta parvula*	female	–	DIVA 3	Atlantic	36.0892° S 49.0267° W	13.07.2009	1500–2000	MF796519	MF796500	MF796467	–	–

accomplished by illustra PuRe-Taq Ready-To-Go PCR Beads (GE Healthcare) using 4 µL of DNA templates in 25-µL reaction volumes. Amplification and sequencing of nuclear ribosomal 18S and mitochondrial cytochrome *c* oxidase subunit I (*COI*) were performed according to Laakmann *et al.* (2013). Nuclear ITS2 was amplified and sequenced using the primers ITS3F (White *et al.*, 1990) and ITS10R (Goetze, 2003) with a thermoprofile of denaturation at 95 °C (5 min) followed by 95 °C (30 s), 55 °C (30 s) and 72 °C (60 s) for 35 cycles and final elongation at 72 °C (7 min). Nuclear ribosomal 28S was amplified using the primers 28S-F1a and 28S-R1a (Ortman *et al.*, 2008) with 94 °C (5 min), 36 cycles of 94 °C (45 s), 50 °C (50 s) and 72 °C (200 s) and final elongation at 72 °C (10 min). Finally, cytochrome *b* (*Cytb*) was amplified using UCYTB151F and UCYTB270R (Merritt *et al.*, 1998), as well as M13-tailed primers, with a thermoprofile of 95 °C (5 min), 40 cycles with 95 °C (30 s), 42 °C (1 min) and 72 °C (1 min), and final elongation at 72 °C (7 min). PCR products were purified using the QIAquick PCR Purification Kit (QIAGEN) and both, PCR products and purified PCR products, were checked on an agarose gel (1%) with GelRed (0.1%). Sequencing was performed at Macrogen, Amsterdam, by using an ABI3730XL automated sequencer and BigDyeTM terminator chemistry.

Using the software GENEIOUS v.7.1.9 created by Biomatters (http://www.geneious.com; Kearse *et al.*, 2012), sequences were assembled, edited and, for *COI* and *Cytb*, checked for reading frames. All new sequences were deposited in GenBank (GenBank Accession numbers MF796440–MF796519; see Table 1). Multiple alignments were performed for the single genes. For 18S and 28S, multiple alignments were performed using MAFFT (Katoh & Standley, 2013), with l-ns option. *COI* and *Cytb* were aligned using MUSCLE v.3.8.1 (Edgar, 2004) with default settings. ITS2 multiple alignments were prepared using RNA salsa (Stocsits *et al.*, 2009). As reference structure of the folding of ITS2 we used the ITS2 structure of *Calanus jashnovi* as a constraint. ITS2 alignment was cut according to the length of *Calanus jashnovi*, downloaded from the ITS2 database with the beginning sequence of 5´- atcaggcagc - 3´ and the ending (according to the analysis by Bradford-Grieve *et al.*, 2017) 5´- ttactttcgac - 3´.

Single and multiple-gene analyses were conducted. For multiple-gene analyses, the different genes were concatenated using GENEIOUS. We analysed two different multiple-gene datasets: (1) we analysed concatenated 18S, 28S, *COI* and *Cytb* together with the dataset on the phylogeny of calanoid superfamilies from Bradford-Grieve *et al.* (2014) based on the results from Blanco-Bercial *et al.* (2011). Multiple alignments of the two converged datasets resulted in aligned fragment lengths for single genes of 931 bp (18S), 733 bp (28S), 547 bp (*COI*) and 327 bp (*Cytb*). The total concatenated fragment was 2541 bp long. (2) We analysed longer fragments of concatenated 18S, 28S, *COI*, *Cytb* and, additionally, ITS2 generated from the Ryocalanoidea and Spinocalanoidea in our study. We used two representatives of the Clausocalanoidea as outgroup taxa: *Paraeuchaeta parvula* (Euchaetidae) and *Prolutamator hadalis* (Aetideidae). This analysis resulted in aligned fragment lengths of the single genes with 1767 bp (18S), 842 bp (28S), 657 bp (*COI*) and 327 bp (*Cytb*). The total concatenated fragment length was 3863 bp.

Concatenated datasets were analysed for best-fit evolutionary models using PartitionFinder 2.0 (Lanfear *et al.*, 2017) with the following parameters: branchlengths = linked, models = all, model_selection = aicc, search = greedy (Lanfear *et al.*, 2012; Lanfear *et al.*, 2017; Guindon *et al.*, 2010). Analyses were run for defined partitions (subsets) with and without regard to the three different codon positions for the mitochondrial genes *COI* and *Cytb*.

Maximum likelihood analyses were performed using RAxML-VI-HPC (Stamatakis, 2006), where only a single model of rate heterogeneity can be applied in partitioned analyses. As recommended in PartitionFinder best scheme results, in case of different models for different subsets, the best rate heterogeneity model was defined by running separate PartitionFinder analyses for each type of rate heterogeneity. The model with the lowest AICc score should be used for the final analysis. In all analyses, GTR+I+G was the model with the lowest AICc scores (see Table 2). Because of the issues regarding the application of the GTR+I+G model (see The RAxML v.8.2.X manual, page 60; Stamatakis, 2014), final analyses were run with the GTRGAMMA nucleotide substitution model and a generation of 10 000 bootstrap replicates.

Bayesian Inference analyses were performed in MrBayes (v.3.2.6; Altekar *et al.*, 2004; Ronquist *et al.*, 2012) using the MrBayes block for partition definitions and best-fit evolutionary model from PartitionFinder best scheme results. However, MrBayes only comprises a small set of evolutionary models for DNA analyses (i.e. nst = 1, nst = 2, nst = 6) and in the case that the recommended model is not included in MrBayes, MrBayes block set best-fit model to GTR (nst = 6), including +I and/or +G (Ronquist *et al.*, 2011). Analyses were run with selected partitions and models (see Table 2) similar to those in Cornils & Blanco-Bercial (2013) and Bradford-Grieve *et al.* (2017), with unlinked parameters for 3 000 000 generations with sampling every 1000 generations. Analyses were checked for Estimated Sample Size (EES) using the software TRACER (v.1.6; Rambaut *et al.*, 2014, available from http://beast.bio.ed.ac.uk/Tracer) and

Table 2. Partitions and substitution models for mulit-gene analyses

Datasets	Partitions/Subsets	Bayesian Inference		Maximum likelihood	
		Best model	Model Block	Model	AICc
Dataset 1	18S = 1–931	GTR+I+G	GTR+I+G (nst = 6 rates = invgamma)	GTR	82607.1647
with Codon	28S = 932–1665	GTR+I+G	GTR+I+G (nst = 6 rates = invgamma)	GTR+G*	75757.3743
	*COI*_pos1 = 1666–2213\3	GTR+I+G	GTR+I+G (nst = 6 rates = invgamma)	GTR+I	78823.9445
	*COI*_pos2 = 1667–2213\3	GTR+I+G	GTR+I+G (nst = 6 rates = invgamma)	GTR+G+I	75659.166
	*COI*_pos3, *Cytb*_pos2 = 1668–2213\3, 2215–2541\3	TRN+I+G	GTR+I+G (nst = 6 rates = invgamma)		
	*Cytb*_pos1 = 2214–2541\3	TVM+G	GTR+G (nst = 6 rates = gamma)		
	*Cytb*_pos2 = 2216–2541\3	GTR+G	GTR+G (nst = 6 rates = gamma)		
Dataset 1	18S = 1–931	GTR+I+G	GTR+I+G (nst = 6 rates = invgamma)	GTR	88643.3451
without Codon	28S = 932–1665	GTR+I+G	GTR+I+G (nst = 6 rates = invgamma)	GTR+G*	77464.7741
	COI = 1666–2213	TIM+I+G	GTR+I+G (nst = 6 rates = invgamma)	GTR+I	82000.7897
	Cytb = 2214–2541	TIM+I+G	GTR+I+G (nst = 6 rates = invgamma)	GTR+G+I	77290.0409
Dataset 2	18S = 1–1767	TRN+I+G	GTR+I+G (nst = 6 rates = invgamma)	GTR	30353.4443
with Codon	28S = 1768–2610	TRN+I+G	GTR+I+G (nst = 6 rates = invgamma)	GTR+G*	29145.3903
	ITS2 = 2611–2877	TVM+I+G	GTR+I+G (nst = 6 rates = invgamma)	GTR+I	29406.6005
	*COI*_pos1 = 2878–3535\3	TRN+I+G	GTR+I+G (nst = 6 rates = invgamma)	GTR+G+I	29101.7244
	*COI*_pos2 = 2879–3535\3	GTR+I	GTR+I (nst = 6 rates = propinv)		
	*COI*_pos3 = 2880–3535\3	TVM+I	GTR+I (nst = 6 rates = propinv)		
	*Cytb*_pos1 = 3536–3863\3	HKY+G	GTR+G (nst = 6 rates = gamma)		
	*Cytb*_pos2 = 3537–3863\3	HKY+G	GTR+G (nst = 6 rates = gamma)		
	*Cytb*_pos3 = 3538–3863\3	GTR+G	GTR+G (nst = 6 rates = gamma)		
Dataset 2	18S = 1–1767	TRN+I+G	GTR+I+G (nst = 6 rates = invgamma)	GTR	32195.291
without Codon	28S = 1768–2610	TRN+I+G	GTR+I+G (nst = 6 rates = invgamma)	GTR+G*	30178.8401
	ITS2 = 2611–2877	TVM+I+G	GTR+I+G (nst = 6 rates = invgamma)	GTR+I	30367.0427
	COI = 2878–3535	GTR+I+G	GTR+I+G (nst = 6 rates = invgamma)	GTR+G+I	30119.7125
	Cytb = 3536–3863	K81UF+I+G	GTR+I+G (nst = 6 rates = invgamma)		

*Chosen model for ML analysis.

for Potential Scale Reduction Factor (PSRF; Gelman & Rubin, 1992). The first 500 trees were discarded as burn-in in the stationary phase, resulting in 2500 trees. Then, the consensus tree (the majority-rule phylogenetic tree) and Bayesian posterior probabilities (BPP) were calculated. Based on p-distances, the pairwise genetic distances were calculated using the software MEGA (v.6; Tamura *et al.*, 2013).

RESULTS

SYSTEMATICS

ORDER CALANOIDA SARS, 1903

SUPERFAMILY RYOCALANOIDEA ANDRONOV, 1974

FAMILY RYOCALANIDAE ANDRONOV, 1974

GENUS *RYOCALANUS* TANAKA, 1956

***RYOCALANUS SQUAMATUS* SP. NOV.**

(FIGS 1–5)

Type material

Holotype: Adult female, dissected, body length 2.17 mm, collection number SMF 37149/1–6 (one vial, five slides); Kurile-Kamchatka trench, 40.5808° N, 150.9833° E, station 9–9, project KuramBio, 23 August 2012, above the sea bed at a depth of 5400 m.

Paratypes: One adult female. Body length 2.05 mm, collection number SMF 37150/1–5 (one vial, four slides); Kurile-Kamchatka trench, 43.0303° N, 152.9758° E, station 7–10, project KuramBio, 17 August 2012, above the sea bed at a depth of 5304 m. One adult male, body damaged, length 1.83 mm, collection number SMF 37151/1–6 (one vial, five slides); Kurile-Kamchatka trench, 41.2000° N, 150.0833° E, station 10–12, project KuramBio, 28 August 2012, above the sea bed at a depth of 5251 m.

Etymology: The specific name refers to the scale-like structures that cover the antennule.

Description: Based on female holotype unless stated otherwise.

Adult female: Total length 2.17 mm; prosome 4.8 times as long as urosome (Fig. 1A, B). Rostrum (Fig. 1C) stout and strong, one-pointed. Cephalosome and pediger 1 partly fused (Fig. 1A), pedigers 4–5 separate; in lateral view, posterolateral corners of prosome extended posteriorly into points, reaching to middle of genital double-somite (Fig. 1A, B). Pedigers 2–5 covered with fine spinules.

Urosome composed of genital double-somite and three articulated somites (Fig. 1A, B, D–H). Genital double-somite slightly asymmetrical, with lateral swelling on left side and ventromedial genital opening; in lateral view genital double-somite swollen ventroanteriorly, seminal receptacles of oval shape. Genital double-somite and urosomites covered with rows of fine spinules (Fig. 1A, B, D–H). Caudal rami symmetrical with two lateral setae (II and III), three terminal setae (IV–VI) and one dorsal seta (VII).

Antennule (Fig. 1I, K) of 24 free segments and extending to pediger 2, covered with scale-like structures. In holotype armature as follows:

I – 2s + 1ae?, II–IV – 5s + 2ae?, V – 2s + 1ae, VI – 2s + 1ae, VII – 2s + 1ae, VIII – 2s + 1ae, IX – 2s + 1ae; X–XI – 4s + 1ae, XII – 1s + 1ae, XIII – 2s, XIV – 2s + 1ae, XV – 1s, XVI – 2s + 1ae, XVII – 2s + 1ae, XVIII – 2s + 1ae, XIX – 2s + 1ae, XX – 2s, XXI – 2s + 1ae, XXII – 1s, XXIII – 1s, XXIV– 2s, XXV – 2s, XXVI – 2s, XXVII–XXVIII – 5s + 1ae.

Antenna (Fig. 2A), coxa with 1, basis with 2 setae; endopod segment 1 with 2 setae, segment 2 with 16 setae; exopod incompletely 8-segmented, with 1, 3, 1, 1, 1, 1, 1, 3 setae.

Mandible (Fig. 2B–D), gnathobase cutting edge with 7 unequal teeth plus ventral seta; exopodal segments with 6 setae; first endopod segment with 2 setae, second with 11 setae; basis with 2 setae. Exopod to endopod ratio 0.82.

Maxillule (Fig. 2E, F), praecoxal arthrite with 9 terminal spines (Fig. 2F), 4 posterior and 2 anterior setae; coxal endite with 6 setae, coxal epipodite with 9 setae; proximal basal endite with 4 setae, distal basal endite with 5 setae; endopod with 15 setae; exopod with 11 setae.

Maxilla (Fig. 2G, H), proximal praecoxal endite bearing 4 setae plus attenuation in holotype, 5 setae plus attenuation in paratype, distal praecoxal endite with 3 setae; coxa without outer seta; coxal endites with 3 setae each; proximal basal endite with 4 setae; endites 2–5 with surface spinules, remaining endopod with 8 setae.

Maxilliped (Fig. 2I), syncoxa with 1 seta on praecoxal endite, 2 setae on proximal coxal endite, 3 setae on middle coxal endite, and 3 setae on distal coxal endite; syncoxa with fine rows of spinules. Basis with 3 distal setae; endopod 6-segmented with 2, 4, 4, 3, 3 and 4 setae.

Legs 1–4 biramous (Fig. 3A–E). Exopods and endopods 3-segmented, except leg 1 endopod 1-segmented and leg 2 endopod 2-segmented. Anterior and posterior surface of legs covered with spinules, these spinules much smaller on anterior surface. Coxa of all legs with surface spinules on inner margin; terminal spines on exopod segment 3 finely serrated. Seta and spine formula as in Table 3. Leg 1 (Fig. 3A), endopod lateral lobe with spinules.

Leg 4 (Fig. 3D), coxa with medial seta (broken in holotype); basis with row of spinules on distal margin; left leg abnormal in holotype (Fig. 3E), lacking lateral

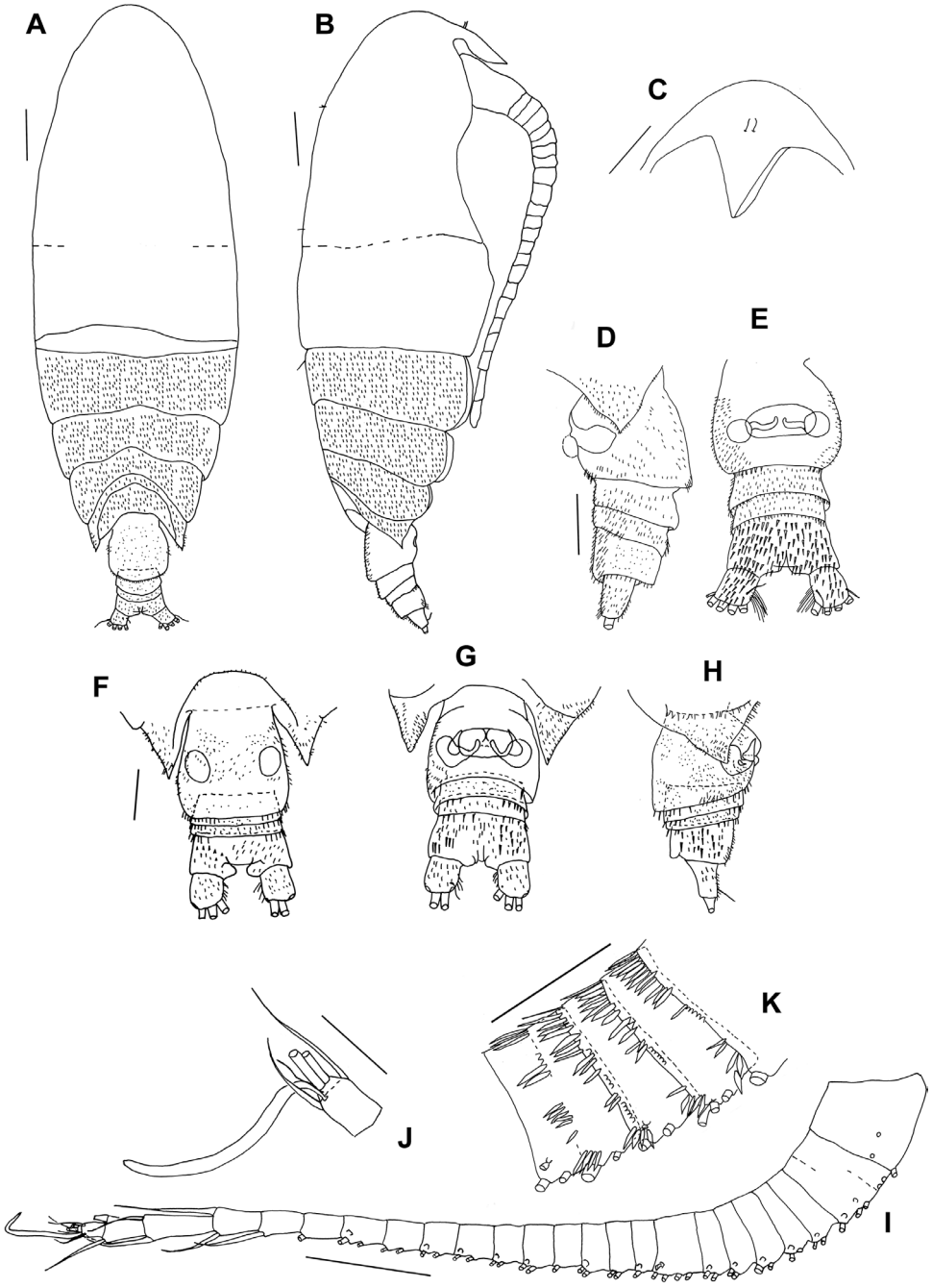

Figure 1. ***Ryocalanus squamatus*** **sp. nov.**, female, holotype (unless otherwise stated). A, habitus dorsal. B, habitus lateral. C, rostrum ventral. D, prosome posterior corners and urosome lateral. E, urosome ventral. F, paratype, prosome posterior corners and urosome, dorsal. G, paratype, prosome posterior corners and urosome ventral. H, paratype, prosome posterior corners and urosome lateral. I, antennule. J, antennule segment XXVII–XXVIII. K, antennule scales on segment VIII–XI. Scale bars: A–I, K: 0.1 mm. J: 0.05 mm.

spines on exopod segment 1 and 3 (no scars), and terminal spine on exopod 3, smaller as right leg.

Adult male: Total length 1.83 mm, prosome 4.6 times as long as urosome (Fig. 4A, B). Rostrum (Fig. 4A, C) stout, strong and one-pointed. Cephalosome and pediger 1 separate (Fig. 4A, B), pedigers 4 and 5 separate. In lateral view, right posterolateral corner of prosome extended posteriorly into points slightly exceeding urosomite 1 (Fig. 4D). Pedigers 2–5 covered

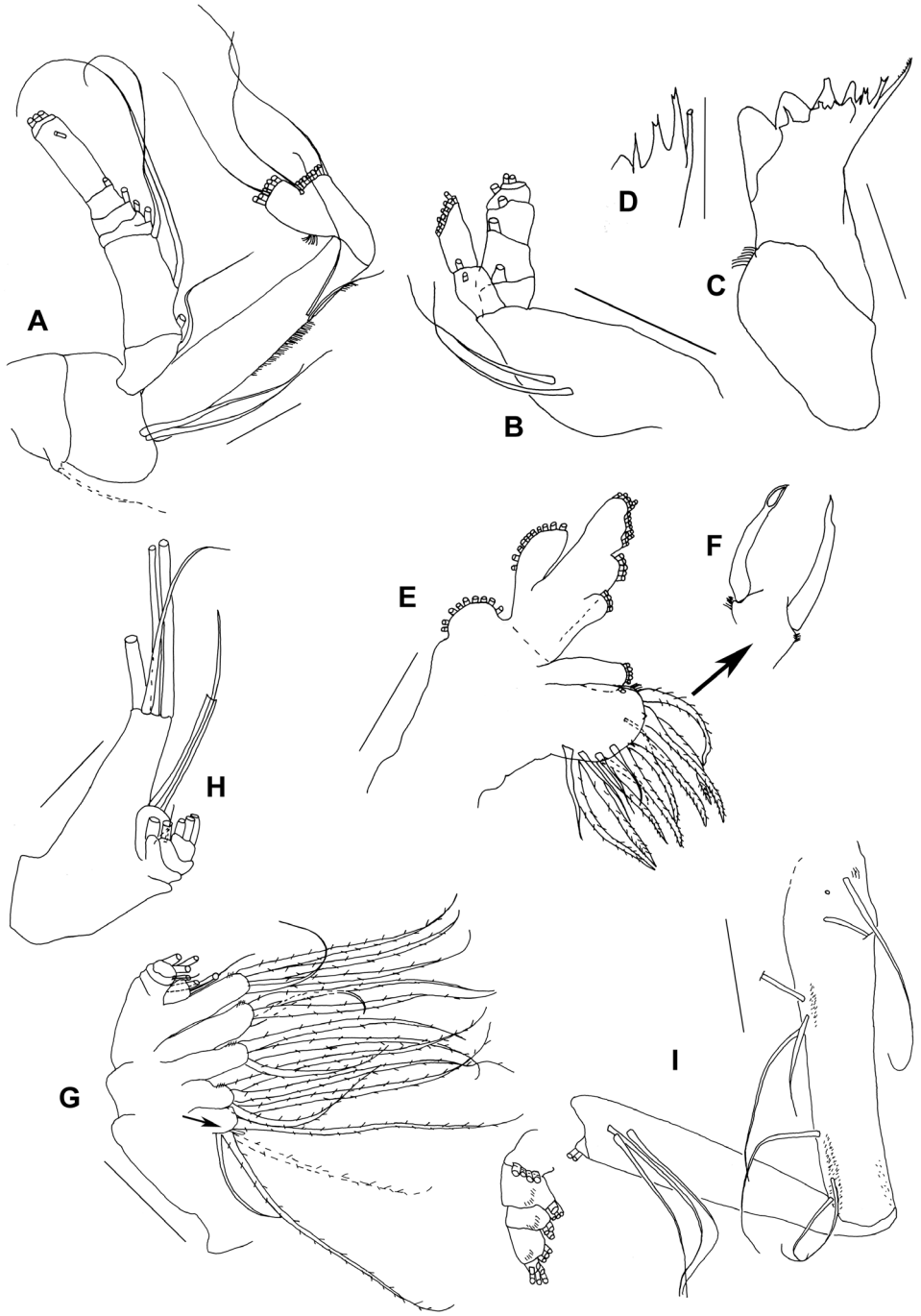

Figure 2. ***Ryocalanus squamatus*** **sp. nov.**, female, holotype (until otherwise stated). A, antenna, dotted seta added after paratype. B, mandible palp. C, mandible gnathobase. D, paratype, mandible gnathobase, cutting edges. E, maxillule. F, paratype, maxillule praecoxal arthrite seta in different positions. G, maxilla. H, paratype, maxilla basal endite and endopod. I, maxilliped. Scale bars: A, H: 0.05 mm. B–D, I: 0.1 mm.

with fine spinules. Caudal rami (Fig. 4B, E) slightly asymmetrical, with one lateral seta (III?), three terminal setae (IV–VI) plus one dorsal seta (VII).

Left antennule (Fig. 4F) unmodified, of 24 free segments, extending to pediger 2, covered with scale-like structures; armature as follows: I – 1s + 1ae, II–IV – 5s + 4ae?, V – 2s + 1ae, VI – 2s + 1ae, VII – 2s + 2ae, VIII – 1s? + 2ae, IX – 2s + 2ae, X–XI – 4s + 4ae, XII – 1s + 1ae; XIII – 2s + 1ae; XIV – 2s + 1ae, XV – 2s + 1ae, XVI – 2s + 1ae, XVII – 2s + 1ae, XVIII – 2s + 1ae, XIX – 2s + 1ae,

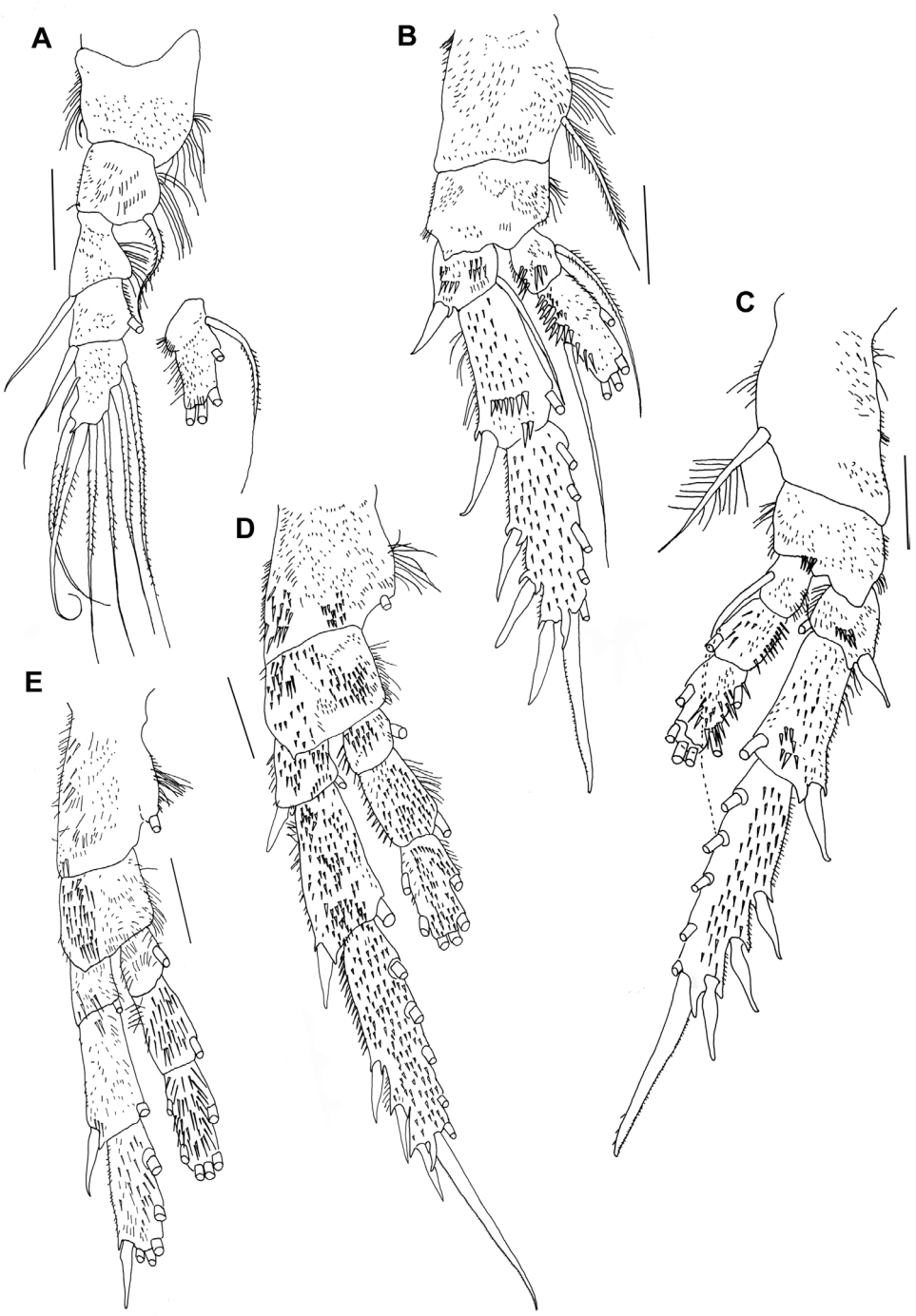

Figure 3. ***Ryocalanus squamatus*** **sp. nov.**, female, holotype. A, leg 1 with endopod figured separately. B, leg 2. C, leg 3. D, leg 4 right. E, leg 4 left. Scale bars: A–E: 0.1 mm.

XX– 2s + 1ae, XXI – 2s + 1ae, XXII – 1s + 1ae, XXIII – 1s + 1ae, XXIV – 2s + 1ae, XXV – 2s + 1ae, XXVI – 2s, XXVII–XXVIII – 4s + 1ae.

Right antennule (Fig. 5A–D) strongly modified for grasping, of 23 free segments; segments XX to XXVI wider than on the left; segments XX to XXII–XXIII with surface spinules; segments XX and XXI with 1 proximal spine each, segment XXV and XXVI with strong lateral attenuations proximally, segment XXII–XXIII fused; hinges occurring between segments XIX

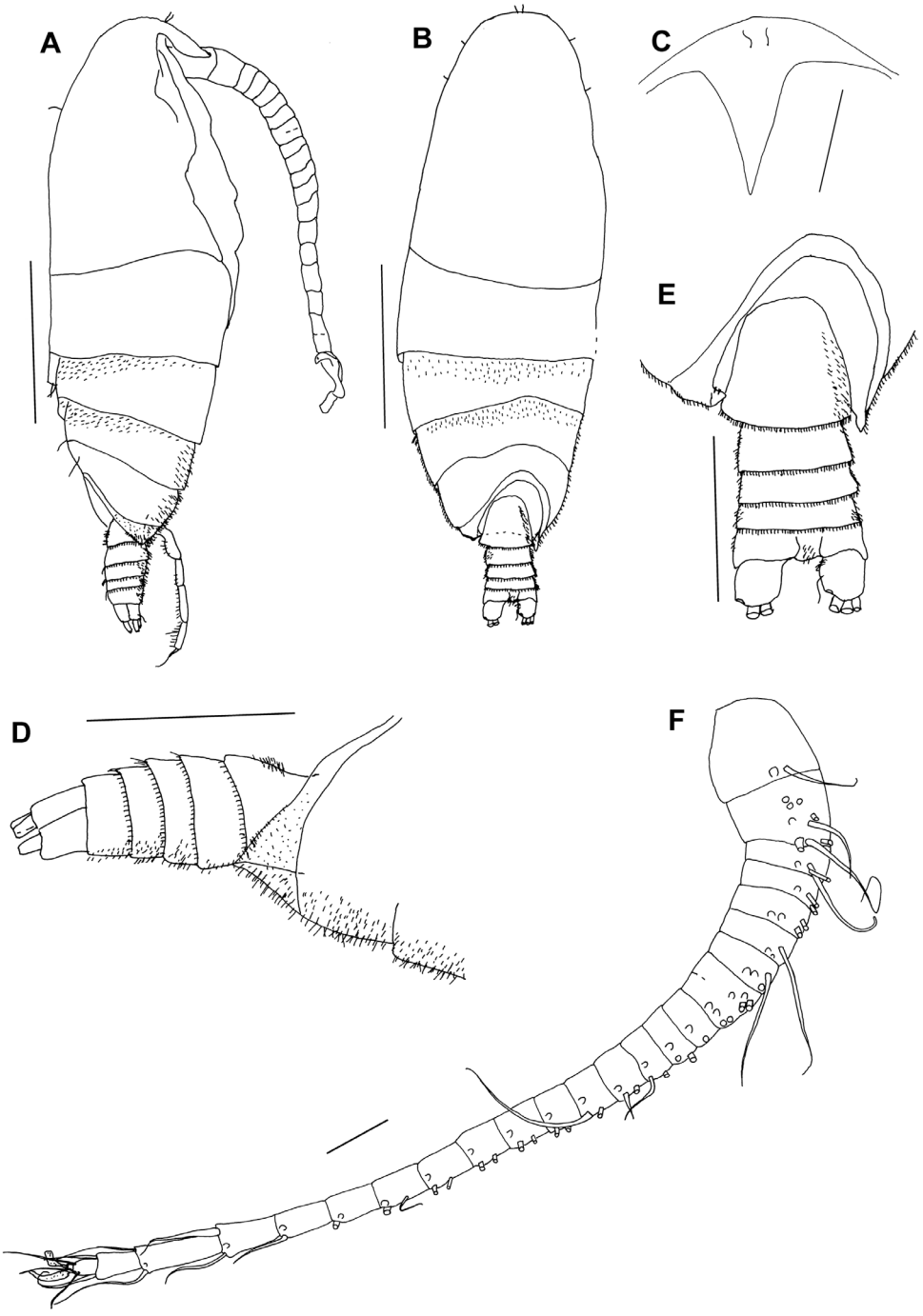

Figure 4. ***Ryocalanus squamatus*** **sp. nov.**, male, paratype. A, habitus lateral. B, habitus dorsal, specimen damaged. C, rostrum ventral. D, urosome lateral. E, urosome dorsal. F, left antennule. Scale bars: A–B: 0.5 mm. C–D, G: 0.1 mm.

and XX, XX and XXI, and XXII–XXIII and XXIV. Armature as follows: segment I – 2s + 1ae, II–IV – 6s + 2ae?, V – 2s + 2ae, VI – 1s + 2ae, VII – 2s + 2ae, VIII – 2s + 2ae, IX – 2s + 2ae; X–XI – 4s + 3ae, XII – 1s + 1ae, XIII – 2s + 1ae, XIV – 2s + 1ae, XV – 1s + 1ae, XVI – 2s + 1ae, XVII – 2s + 1ae, XVIII – 2s + 1ae, XIX – 2s + 1ae, XX – 1s+ 1ae + spine, XXI – 1s + 1ae + spine, XXII–XXIII – 2s + 1ae, XXIV – 2s, XXV – 2s + 1ae + strong, attenuation, XXVI – 2s + strong, spine like attenuation, XXVII–XXVIII – 5s + 1ae.

Antenna, mandible and maxillule similar to those of female. Maxilla as in female, with proximal praecoxal endite bearing 4 or 5 setae, but without attenuation.

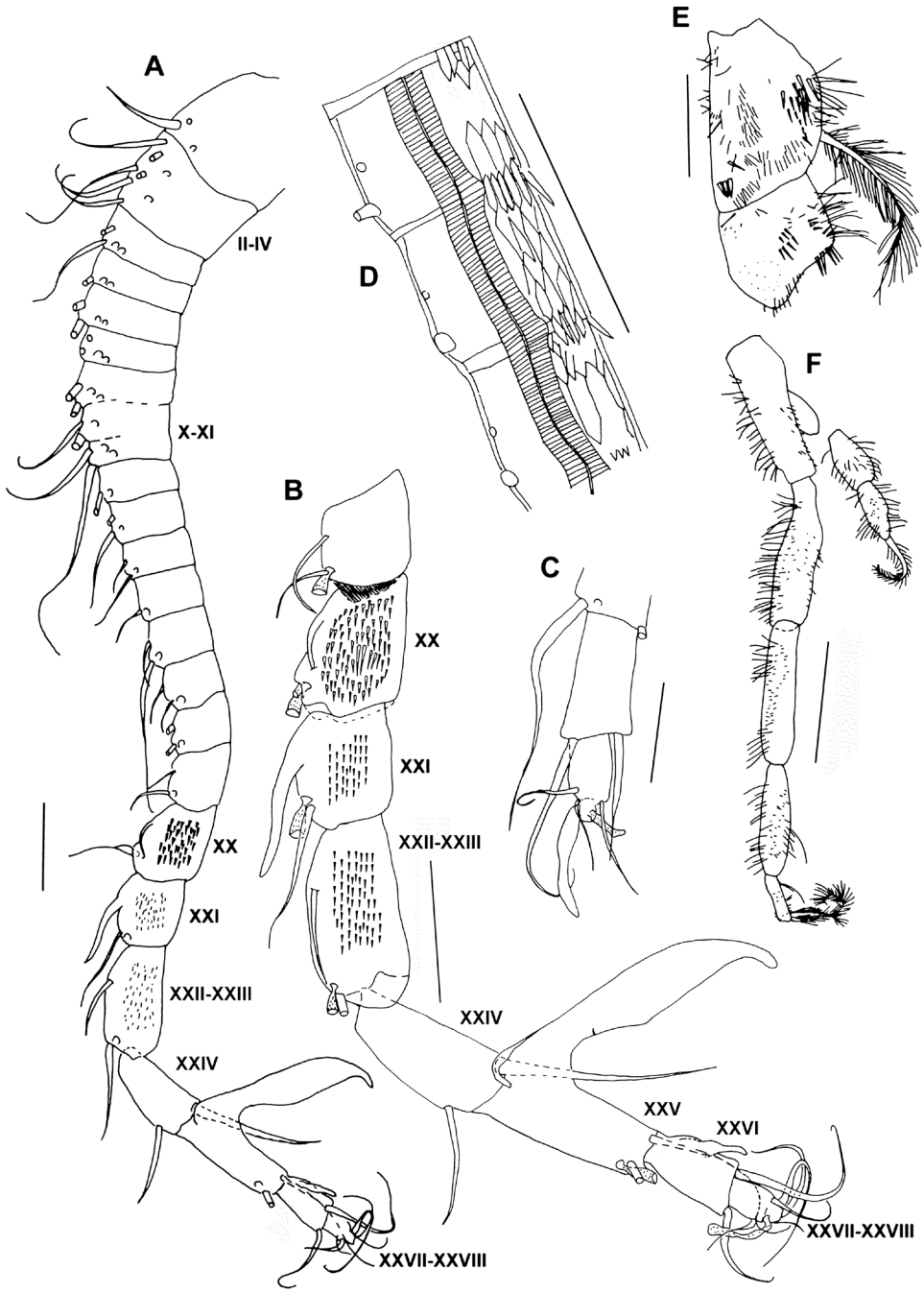

Figure 5. ***Ryocalanus squamatus*** **sp. nov.**, male, paratype. A, right antennule. B, right antennule, segments XIX–XXVIII. C, right antennule, segments XXVI–XXVIII. D, right antennule, segments XVII–XIX, different position. E, P4, coxa and basis. F, leg 5. Scale bars: A–B, D–F: 0.1 mm. C: 0.05 mm.

Maxilliped similar to that of female.

Legs 1–4 similar to those of female, but less spinulose. Leg 2 one leg abnormal, lacking lateral spines on exopod segment 1 and 2 (no scars), and terminal spine on exopod 3, exopod 3 with 7 setae, leg small. Leg 4 coxa without strong spinules (Fig. 5E). Leg 5 (Fig. 5F) uniramous on both sides, covered with rows of spinules on posterior surface. Right leg with 1-segmented exopod, shorter than left leg, with terminal spine. Left leg with 3-segmented exopod, terminal segment with two spines.

Remarks: The new species shares the main morphological characters with species of the genus *Ryocalanus* (Renz *et al.*, 2013), which is a 1-pointed

Table 3. Seta and spine formula of ***Ryocalanus squamatus* sp. nov** from the Kurile-Kamchatka trench

Leg 1	coxa 0-0	basis I-1	exp I-0; I-1; 2, 1, 4
			enp 0, 2, 3
Leg 2	coxa 0-1	basis 0-0	exp I-1; I-1; III, I, 5
			enp 0-1; 1, 2, 2
Leg 3	coxa 0-1	basis 0-0	exp I-1; I-1; III, I, 5
			enp 0-1; 0-1; 2, 2, 2
Leg 4	coxa 0-1	basis 0-0	exp I-1; I-1; III, I, 5
			enp 0-1; 0-1; 2, 2, 2

rostrum, the armament of the female antennule ancestral segment XXII with 1 seta, a leg 1 endopod with a proximal inner wedge-shaped projection and a male antennule with ancestral segments XXI/XXII–XXIII fused. Both sexes are known only for *R. brasilianus* Renz, Markhaseva & Schulz, 2013, while *R. spinifrons* Shimode, Toda & Kikuchi, 2000 is only known from females and *R. bowmani* Markhaseva & Ferrari, 1996 and *R. infelix* Tanaka, 1956 are represented only by males (female of *R. infelix* is described herein).

Ryocalanus squamatus sp. nov. differs from all other *Ryocalanus* species by the shape of the rostrum, which is short and stout, compared to the long and slender rostrum possessed by all other *Ryocalanus* species and an only slightly asymmetrical genital segment, which is strongly asymmetrical in *R. brasilianus*, *R. spinifrons* and *R. infelix*. Pedigers 2–5, as well as the anterior part of the legs, are covered in fine spinules, which are absent in other *Ryocalanus* females, and the coxa of leg 4 lacks the robust spines that are usually found in all other ryocalanid females of the genera *Ryocalanus* and *Yrocalanus*. The antennule is covered with scale-like structures, a character not detected so far in any other species of *Ryocalanus*.

There are significant morphological transformations in the *Ryocalanus* male right ancestral antennule segments distal to segment XIX, and evidence that ancestral segments XXI/XXII–XXIII are fused, with the main hinge located between fused segments XXII–XXIII and segment XXIV. This is unlike the earlier interpretation of the *R. infelix* male right antennule (Ohtsuka & Huys, 2001). Consequently, the male right antennules of *Ryocalanus* species are distinct to the male right antennules in the genus *Yrocalanus*, where the main hinge can be found between segment XXII and fused segments XXIII–XXIV. For further comments, see also remarks for the description of a *R. infelix* female with additional comments for the male. The right male antennule of *Ryocalanus squamatus* sp. nov. differs from that of other *Ryocalanus* males in the shape of segment XXV, which has a strong lateral attenuation, being longer than the segment itself. This attenuation is absent in other *Ryocalanus* species. Furthermore, segments XX–XXIII are equipped with surface spinules in *R. squamatus* sp. nov., while present on segments XIX–XXIII in *R. infelix* (Tanaka, 1954) and segments XIV–XXI in *R. brasilianus* (Renz *et al.*, 2013). These spinules are lacking in the *R. bowmani* male right antennule. The lateral teeth observed on the male antennule segments XXVI and XXIV in *Ryocalanus infelix* and *R. brasilianus* and the combed spines on segments XXIV and XXV in *R. bowmani* are absent in *R. squamatus* sp. nov..

The antenna exopod to endopod ratio in the new species is 0.82, while in all other *Ryocalanus* species it is close to 1, a character hypothesized to be diagnostic for the genus *Ryocalanus* (Renz *et al.*, 2013). The mandible basis carries 2 setae (vs. 3 setae in all other *Ryocalanus* species), the mandible first endopod segment carries 2 setae (vs. 4 setae in all other *Ryocalanus* species) and the maxilliped endopod segment 5 outer seta is missing (this seta is present in all other species).

Males of *Ryocalanus squamatus* sp. nov. differ from their congeers in the shape of the rostrum, the spinules covering pedigers 2–5 and the scale-like structures covering the antennule (the latter two not present in other *Ryocalanus* species), the shape of ancestral segments on the right antennule with a large, hook-like extension on the posterior border of ancestral segment XXV, and the number and morphology of spines and segments of leg 5. From the armature of the 2-segmented right leg 5 it cannot be distinguished if the segments comprise a fused coxo- and basipodite with a one-segmented exopod or if the exopod is reduced.

Some variability was observed in the armature of the proximal praecoxal endite of the maxilla between right and left limb of individuals in both female and male specimens, i.e. the presence of 4 or 5 setae. Furthermore, this endite was always equipped with a short attenuation in females, a feature not reported before in other ryocalanid species. However, a re-examination of the holotype of *Yrocalanus bicornis* (Markhaseva & Ferrari, 1996) (Smithsonian Institution, Catalogue No. USNM 264034, as *Ryocalanus bicornis* Markhaseva & Ferrari, 1996) showed that this short attenuation was present in the type material from Volcano 7. In both sexes of *R. squamatus* sp. nov., the distal spine on the maxillule praecoxal arthrite had a cavity at its tip, presumably a specific adaptation connected with feeding. This character was also found during the re-examination of the holotype of *Ryocalanus bowmani* from Volcano 7 (Smithsonian Institution, Catalogue No. USNM 268291; Fig. 6). A morphologically similar structure can be found in the mandible of Heterorhabdidae, although it is not clear from the analysis by light microscopy if this structure serves the same function during predatory feeding as suggested for this family (Ohtsuka *et al.*, 1997).

Abnormalities were observed in the formation of a swimming leg of *Ryocalanus squamatus* sp. nov., as

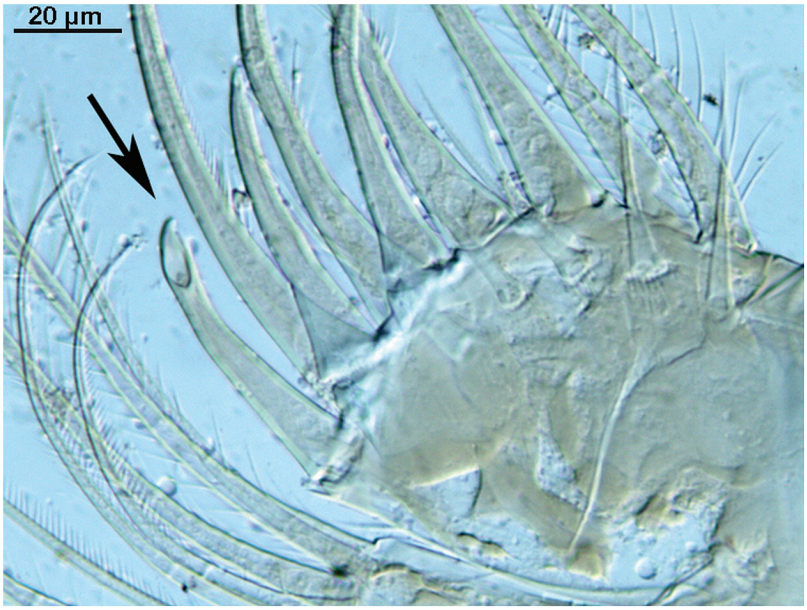

Figure 6. *Ryocalanus bowmani* Markhaseva & Ferrari, 1996 (Smithsonian Institution, Catalogue Nr. USNM 268291), maxillule praecoxal arthrite.

in one female, as well as the male specimen, exopods of leg 4 and 2, respectively, lacked lateral spines, and exopod segment 3 lacked the terminal spine and deviated in the setation typical for this taxon.

RYOCALANUS INFELIX TANAKA, 1956 (FIGS 7–10)

Material: Adult female, dissected, body length 2.65 mm, collection number SMF 37152/1–6 (one vial, five slides); Kurile-Kamchatka trench, 46.2333° N, 155.5333° E, station 2–10, project KuramBio, 3 August 2012, above the sea bed at a depth of 4865 m. One adult female, dissected, body length 2.60 mm, collection number SMF 37153/1–4 (one vial, three slides); Kurile-Kamchatka trench, 43.0166° N, 152.9666° E, station 7–10, project KuramBio, 17 August 2012, above the sea bed at a depth of 5223 m. One adult male, dissected, body length 2.11 mm, collection number SMF 37154/1–4 (one vial, three slides); Kurile-Kamchatka trench, 43.5666° N, 153.9666° E, station 5–10, project KuramBio, 11 August 2012, above the sea bed at a depth of 5375 m. One adult male, dissected, body length 2.11 mm, collection number SMF 37155/1–3 (one vial, two slides); Kurile-Kamchatka trench, 46.2333° N, 155.5333° E, station 2–10, project KuramBio, 3 August 2012, above the sea bed at a depth of 4865 m.

Description: Based on two females and two males.

Adult female: Total length 2.65 mm; prosome 5.1 times as long as urosome (Fig. 7A, B). Rostrum (Fig. 7A, C) one-pointed, slender. Cephalosome and pediger 1 separate (Fig. 7A, B), pedigers 4–5 separate; in dorsal view posterolateral corners of prosome asymmetrical, extended posteriorly into points, extending to distal margin of genital double-somite on right side and to distal margin of second urosomal segment on left side (Fig. 7A, B, D). Ventral inner surface of pediger 5 with short spinules.

Urosome composed of genital double-somite and three articulated or partly articulated somites (Fig. 7D–G). Genital double-somite asymmetrical, with lateral swelling on right side or left side and faint line of incomplete fusion on dorsal and ventral surface; in lateral view swollen ventromedially, seminal receptacles in lateral view oval, turned upward. Urosomites 2, 3 and 4 asymmetrical, 3 and 4 partly fused. Urosome covered by viscous mass. Caudal rami asymmetrical with right ramus longer and wider than left; both rami with row of spinules on inner margin and with two lateral setae (II and III), three terminal setae (IV–VI) and one dorsal seta (VII).

Antennule (Fig. 7H) of 24 free segments, armature as follows:

I – 1s + 1ae, II–IV – 6s + 4ae, V – 2s + 2 ae, VI – 2s + 1ae, VII – 2s + 2ae, VIII – 2s + 2ae, IX – 2s + 2ae; X–XI – 4s + 4ae, XII – 1s, XIII – 2s + 2ae; XIV – 2s, XV – 1s + 1ae, XVI – 2s + 1ae, XVII – 2s + 1ae, XVIII – 2s + 1ae, XIX – 2s, XX – 2s + 1ae, XXI – 2s, XXII – 1s, XXIII – 1s, XXIV – 2s, XXV – 2s, XXVI – 2s, XXVII–XXVIII – 4s + 1ae.

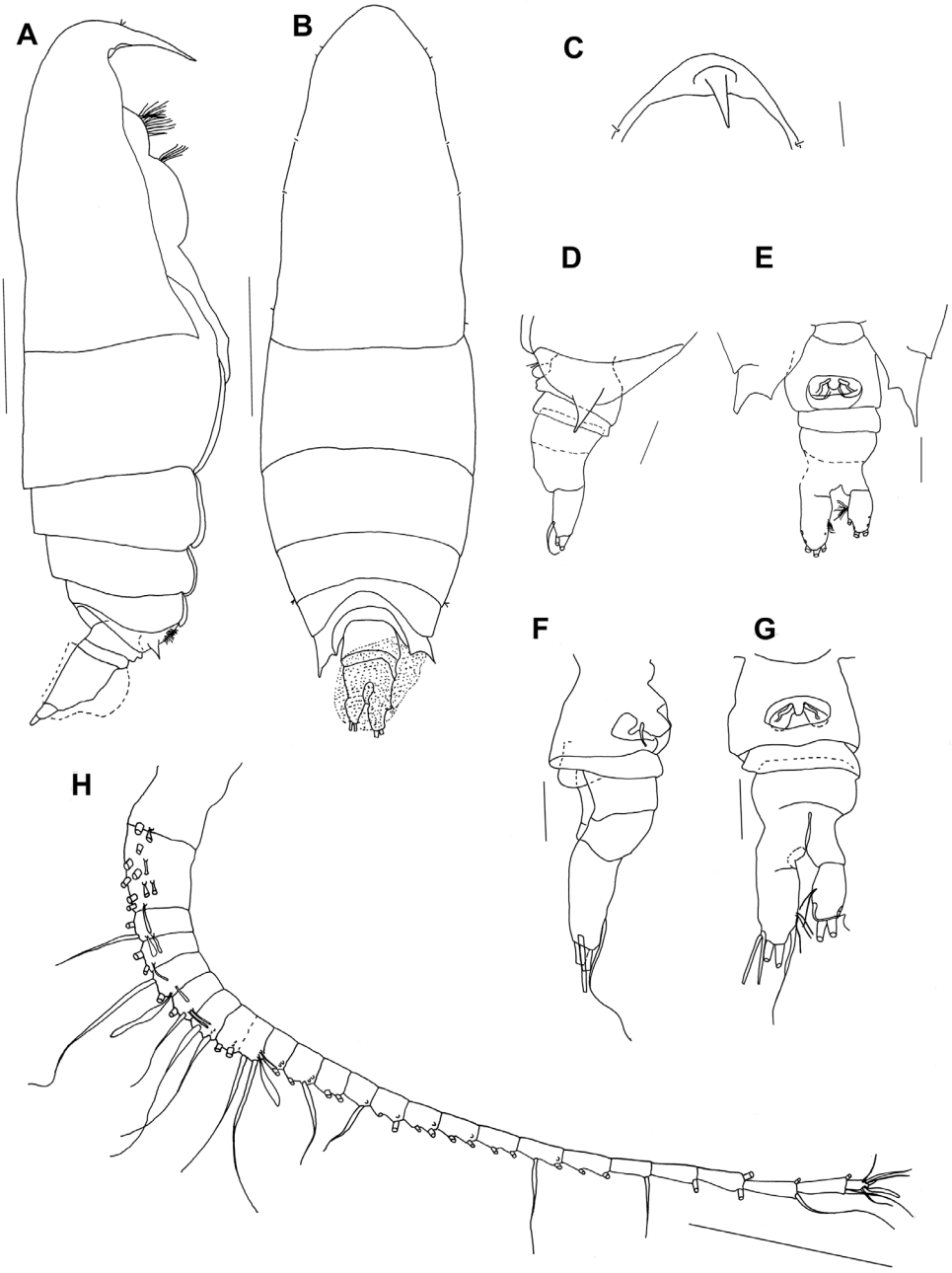

Figure 7. *Ryocalanus infelix* Tanaka, 1956, female. A, habitus lateral. B, habitus dorsal. C, rostrum ventral. D, urosome lateral. E, prosome posterior corners and urosome ventral F, urosome lateral. G, urosome ventral. H, antennule. Scale bars: A–B: 0.5 mm. C–G: 0.1 mm.

Antenna (Fig. 8A), coxa with 1, basis with 2 setae; endopod segment 1 with 2 setae and row of spinules, segment 2 with 16 setae; exopod 8-segmented, with 1, 3, 1, 1, 1, 1, 1, 3 setae.

Mandible (Fig. 8B), gnathobase cutting edge with 8 unequal teeth plus ventral seta; basis with 3 setae; exopodal segments incompletely fused, with 6 setae; first endopod segment with 4 setae (3 setae plus 1 scar), second with 11 setae.

Maxillule (Fig. 8C), praecoxal arthrite with 9 terminal spines, 3 posterior and 1 anterior setae; posterior surface of praecoxal arthrite with small spinules; coxal endite with 6 setae, coxal epipodite setae broken in all specimens; proximal basal endite with 4 setae, distal basal endite with 5 setae and small surface spinules; endopod with 12 setae and patch of small surface spinules; exopod with 8 setae.

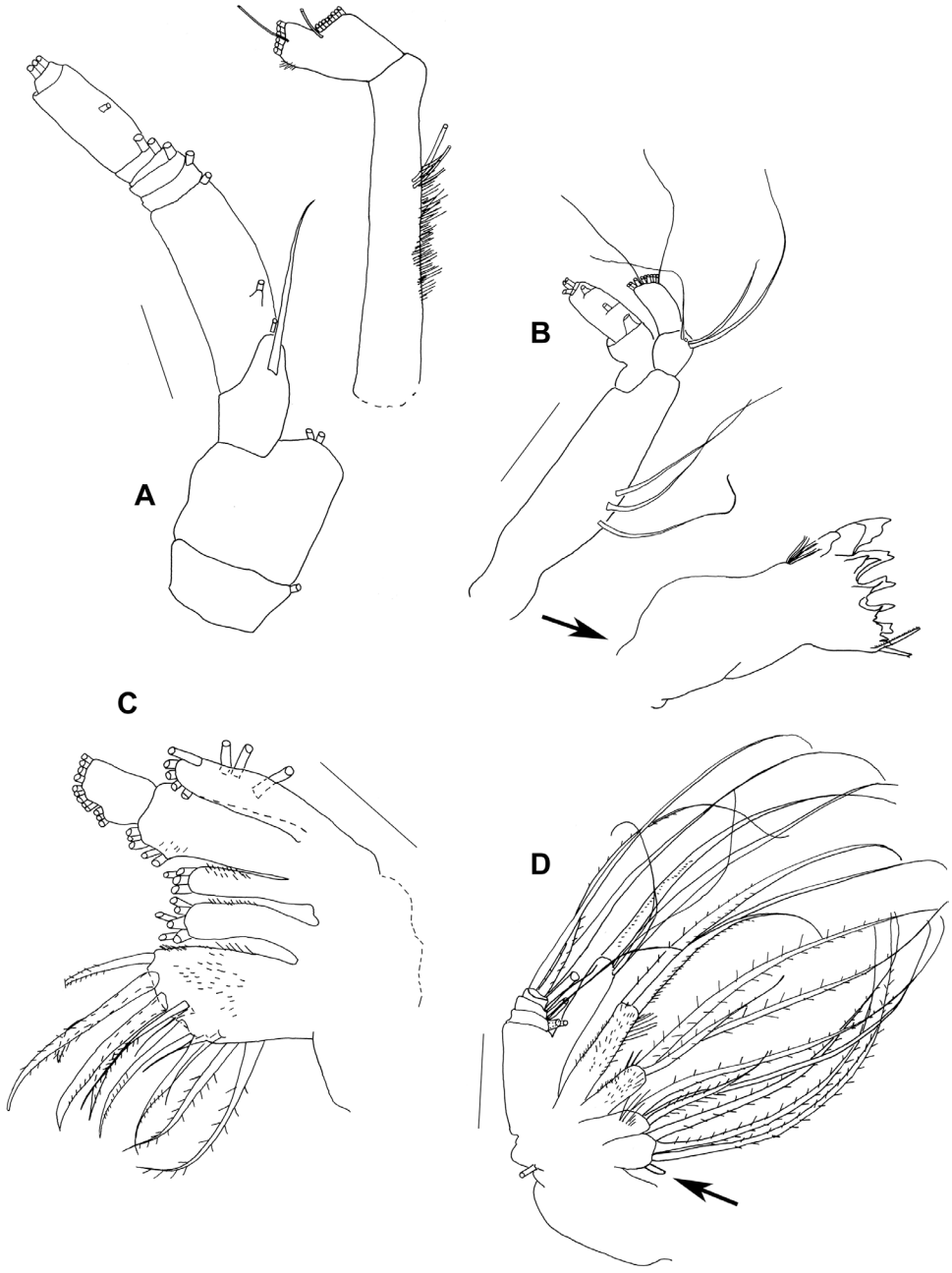

Figure 8. *Ryocalanus infelix* Tanaka, 1956, female. A, antenna. B, mandible. C, maxillule. D, maxilla. Scale bars: A–D: 0.1 mm.

Maxilla (Fig. 8D), proximal praecoxal endite bearing 3 setae plus attenuation on left limb, 5 setae in right limb, distal praecoxal endite with 3 setae and surface spinules; coxa with 1 outer seta; coxal endites with 3 setae each and surface spinules; proximal basal endite 4 setae; remainig endopod with 9 setae.

Maxilliped (Fig. 9A), syncoxa with 1 seta on proximal praecoxal endite, 2 setae on middle endite, and 3 setae on distal praecoxal endite; coxal endite with 3 setae; basis with 3 medial setae; endopod 6-segmented with 2, 4, 4, 4, 3 + 1, and 4 setae.

Legs 1–4 biramous (Fig. 9B–E) with 3-segmented exopods, endopod 1-segmented in leg 1, 2-segmented in leg 2 and 3-segmented in legs 3–4. All endopod and exopod segments with rows of spinules on posterior surface. Coxa of legs 1–3 with inner surface spinules. Leg 2 and 3 with finely serrate terminal spine on exopod segment 3. Seta and spine formula as in Table 4. Leg 1

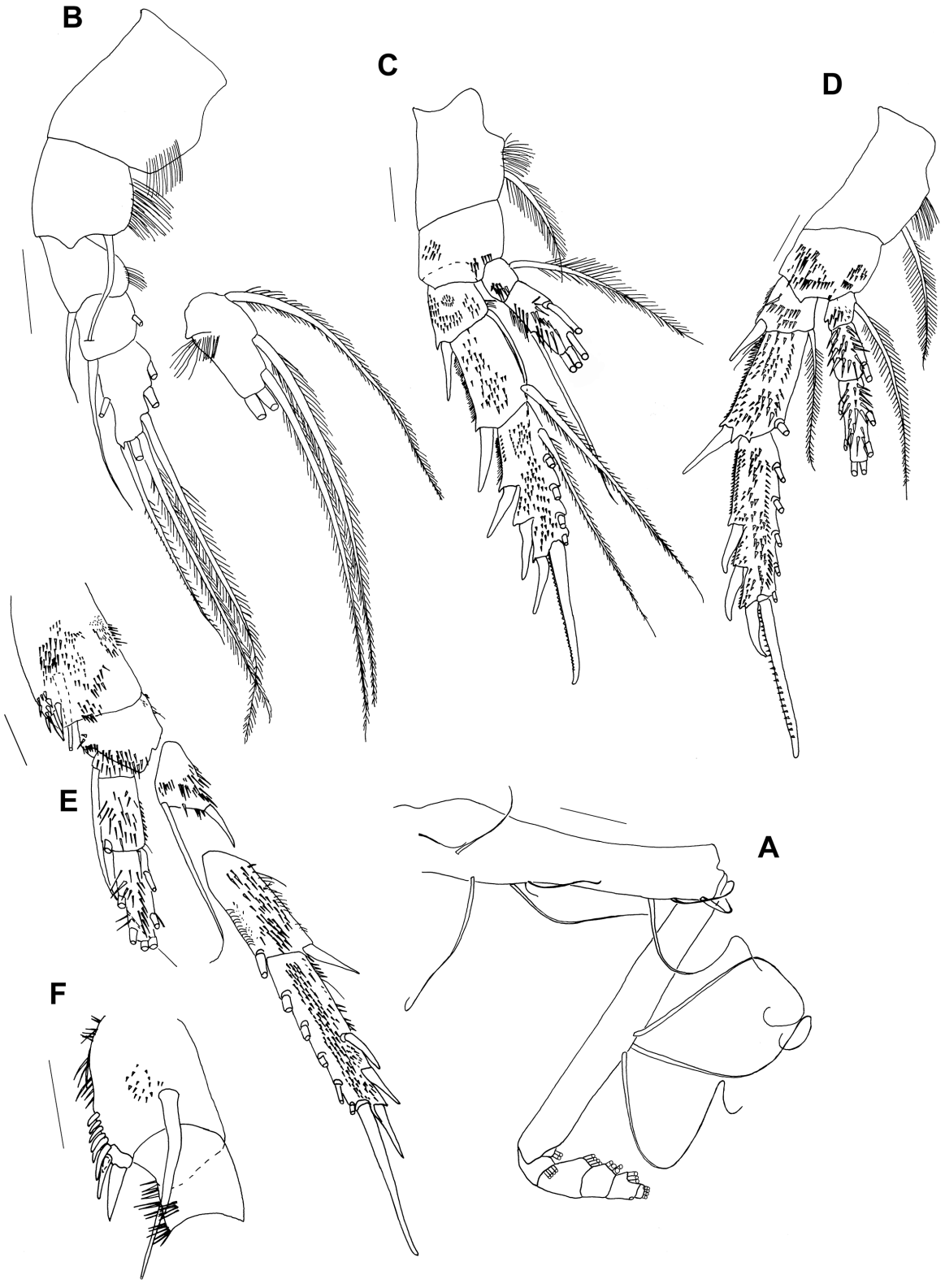

Figure 9. *Ryocalanus infelix* Tanaka, 1956, female. A, maxilliped. B, leg 1 with endopod figured separately. C, leg 2. D, leg 3. E, leg 4 with exopod figured separately. F, leg 4 coxa and basis, different view. Scale bars: A–F: 0.1 mm.

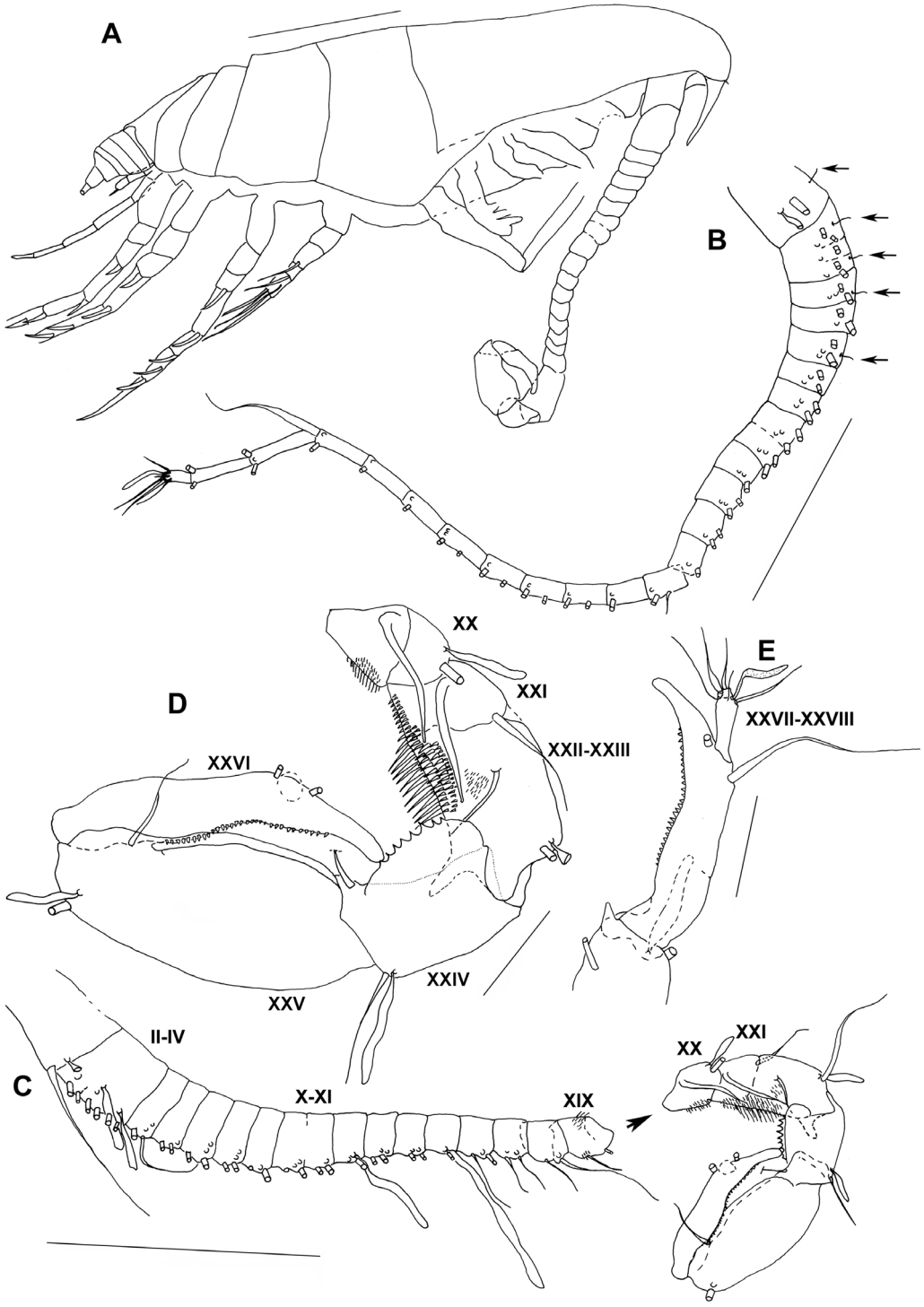

Figure 10. *Ryocalanus infelix* Tanaka, 1956, male. A, habitus lateral. B, antennule left. C, antennule, right, segments XX–XXVIII figured separately. D, antennule, right, segments XX–XXVI. E, antennule, segment XXV–XXVIII. Scale bars: A–C: 0.5 mm. D–E: 0.1 mm.

(Fig. 9B), endopod lateral lobe with spinules and inner wedge-shaped projection; exopod segment 1 with lateral spine (broken in one specimen) and inner spinules, segment 2 with long lateral spine about the length of exopod segment 2 and 3 together, segment 3 with terminal spine, broken in one specimen.

Table 4. Seta and spine formula of *Ryocalanus infelix* Tanaka, 1956 from the Kurile-Kamchatka trench

Leg 1	coxa 0-0	basis 0-1	exp I-0; I-1; 2, 1, 4
			enp 0, 2, 3
Leg 2	coxa 0-1	basis 0-0	exp I-1; I-1; III, I, 5
			enp 0-1; 1, 2, 2
Leg 3	coxa 0-1	basis 0-0	exp I-1; I-1; III, I, 5
			enp 0-1; 0-1; 2, 2, 2
Leg 4	coxa 0-1	basis 0-0	exp I-1; I-1; III, I, 5
			enp 0-1; 0-1; 2, 2, 2

Leg 2 (Fig. 9C), coxa with medial seta.

Leg 4 (Fig. 9E, F), coxa with inner surface spinules, 1 strong and 8 short distolateral spines, and patches of spinules on posterior surface.

Adult male: Total length 2.11 mm (Fig. 10A). Oral limbs and swimming legs as in original description by Tanaka (1956), deviating only in following details:

Left antennule (Fig. 10B) unmodified, of 24 free segments, extending to first urosome segment; armature as follows: I – 1s + 1ae, II–IV – 5s + 3ae? + 2 short sensillae (Fig. 10B, see arrows), V – 2s + 2ae + 1 short sensilla, VI – 2s + 1ae, VII – 2s + 2ae + 1 short s in particular position, VIII – 2s + 2ae, IX – 2s + 2ae, X–XI – 4s + 4ae, XII – 1s + 2ae; XIII – 2s + 2ae; XIV – 2s + 1ae, XV – 1s + 1ae, XVI – 2s + 1ae, XVII – 1s + 1ae, XVIII – 2s + 1ae, XIX – 2s + 1ae, XX – 2s + 1ae, XXI – 2s + 1ae, XXII – 1s + 1ae, XXIII – 1s + 1ae, XXIV – 2s + 1ae, XXV – 2s + 1 ae, XXVI – 2s, XXVII–XXVIII – 4s + 1ae.

Right antennule (Fig. 10C–E) strongly modified for grasping, of 22 free segments; segments XVIII–XXII/XXIII with surface spinules; segments XIX–XXVI strongly enlarged; segments XX and XXI with 1 proximal spine each, segments XXI–XXII partly fused, segments XXII–XXIII fused, segment XXIV with lateral broad denticulated lamella, segment XXV with small lateral chitinized lamella; hinges occurring between segments XVIII and XIX, XIX and XX, XX and XXI, XXIII and XXIV, XXIV and XXV and XXIV and XXV. Armature as follows: segment I – 1s + 1ae, II–IV – 6s + 4ae, V – 2s + 2ae, VI – 2s + 1ae, VII – 2s + 2ae, VIII – 2s + 2ae, IX – 2s + 1ae; X–XI – 4s + 3ae, XII – 1s + 2ae, XIII – 2s + 2ae, XIV – 2s + 1ae, XV – 1s + 1ae, XVI – 2s + 1ae, XVII – 2s + 1ae, XVIII – 2s + 1 ae, XIX – 2s, XX – 1s+ 1ae +1 spine, XXI – 1s +1 spine, XXII–XXIII – 2s + 1ae, XXIV – 2s + 1ae, XXV – 2s + 1ae, XXVI – 2s, XXVII–XXVIII – 5s + 1ae.

Remarks: Ryocalanus infelix was so far only known from a male specimen. Together with female specimens, also males of this species were present in the samples. *COI* sequence analysis verified the assignment of females and males to the same species (see below).

The urosome of all female specimens was covered by a viscous mass (as indicated in Fig. 7A, B) that was only removable by placing the urosome into lactic acid for at least 24 h. We hypothesize that this viscous mass-like structure is either connected to the mating process or might be remnants of egg sacs. The antennule of one female did show a quadrithek arrangement of appendages with segments V, VII, VIII, IX and XIII bearing two small, slender aesthetascs in addition to two setae. While the doubling of aesthetascs is unusual in female calanoid copepods, it has previously been observed in a few genera within the Calanidae by Fleminger (1985). He postulated that quadrithek females derive from genotypic males in which the gonad develops as an ovary and suggested that environmental factors or internal factors affect the final, phenotypic sex.

The morphology of the male specimens is mostly as in the original description of Tanaka (1956), except for: the basis of leg 1 carries 1 medial seta that is missing in the original description; the maxillule coxal endite carries 6 setae (vs. 5 setae in the original description); and the maxillary endopodite carries 9 setae (vs. 8 setae in the original description). The setation of the left male antennule, which was missing in the original description, is given here. Segmental fusions in the right male antennule are not absolutely unambiguous in *Ryocalanus infelix* and *R. squamatus* sp. nov. due to the significant *Ryocalanus* male morphological transformations in the ancestral antennule segments distal to the segment XXI. More specifically, a fusion of segment XXV–XXVI, observed for *R. infelix* (Tanaka, 1956), could not be observed here. Instead, based on the morphology of the male antennules of *Ryocalanus squamatus* sp. nov. and *R. infelix* from the Kurile-Kamchatka trench, ancestral segments XXII and XXIII are apparently fused. This compund segment (XXII–XXIII) is distally followed by segments that are each supplied by two setae (both distoanterior and distoposterior), which is a marker for the ancestral segments XXIV, XXV, XXVI and XXVII (e.g. Huys & Boxshall, 1991). This interpretation can also be applied to *R. brasilianus* (Renz *et al.*, 2013), for which the earlier interpretation of antennule segmental fusions was left for discussion. The right antennule of *R. infelix* differs from other *Ryocalanus* species in the shape of the denticulated and chitinized lamella on segments XXIV and XXVI, which is of a different structure in *R. brasilianus* (Renz *et al.*, 2013) and absent in *R. squamatus* sp. nov. and *R. bowmani* (Markhaseva & Ferrari, 1996).

The length of males discovered from the Kurile-Kamchatka trench varied between 1.95 and 2.15 mm.

Females and males differed in the number of setae in the mandible endopod segment 2 (10 in males, 11 in

females), the maxilla basal distal endite setation (four in females, three in males) and the maxilliped endopod setation (endopod 6-segmented with 2, 4, 4, 4, 3 + 1, and 4 setae in females, endopod 6-segmented, with 2, 4, 3, 2, 2 + 1, and 4 setae in males). The maxilla praecoxal endite showed variations in setation between left and right limbs of both, female and male individuals with the armament being 3 setae plus attenuation or 5 setae.

GENUS *YROCALANUS* RENZ, MARKHASEVA & SCHULZ, 2013

YROCALANUS KURILENSIS SP. NOV.

(FIGS 11–14)

Type material

Holotype: Adult female, dissected, body length 1.75 mm, collection number SMF 37156/1–5 (one vial, four slides); Kurile-Kamchatka trench, 43.5666° N, 153.9666° E, station 5–10, project KuramBio, 11 August 2012, above the sea bed at a depth of 5376 m.

Paratypes: One adult female, body length 1.75 mm, collection number SMF 37157/1–4 (one vial, three slides); Kurile-Kamchatka trench 42.2333° N, 151.7000° E, station 9–9, project KuramBio, 20 August 2012, above the sea bed at a depth of 5125 m.

One adult male, body length 1.58 mm, collection number SMF 37158/1–6 (one vial, five slides); Kurile-Kamchatka trench, 46.2333° N, 155.5333° E, station 2–9, project KuramBio, 3 August 2012, above the sea bed at a depth of 4863 m.

One adult male, body length 1.53 mm, collection number SMF 37159/1–5 (one vial, four slides); Kurile-Kamchatka trench, 46.9740° N, 157.3048° E, station 1–11, project KuramBio, 30 July 2012, above the sea bed at a depth of 5418 m.

Etymology: The specific name is derived from the location of collection, the Kurile-Kamchatka trench.

Description: Based on female holotype unless otherwise stated.

Adult female: Total length 1.75 mm; prosome 4.6 times as long as urosome (Fig. 11A, B). Rostrum (Fig. 11A, C) two-pointed. Cephalosome and pediger 1 partly fused (Fig. 11A, B), pedigers 4–5 separate; in lateral view posterolateral corners of prosome extended posteriorly into points, reaching distal margin of the genital double-somite. Urosome composed of genital double-somite and three articulated somites (Fig. 11D, E). Genital double-somite symmetrical, with short spinules distolaterally on right side and ventromedial genital opening; in lateral view seminal receptacles elongated, turned upward. Dorsal posterior margins of genital double-somite to third urosomal somite each with row of spinules (Fig. 11D). Caudal rami symmetrical, with row of spinules on inner margin and with two lateral setae (II and III), three terminal setae (IV–VI) and one dorsal seta (VII).

Antennule (Fig. 11F) of 24 free segments and extending to distal border of pediger 2. In holotype armature as follows:

I – 2s + 1ae, II–IV – 4s + 3?, V – 2s + 1ae, VI – 2s, VII – 2s + 1ae, VIII – 2s, IX – 2s + 1ae; X–XI – 4s + 1ae?, XII – 1s + 1ae, XIII – 2s + 1ae, XIV – 2s + 1ae, XV – 1s + 1ae, XVI – 2s + 1ae, XVII – 2s + 1ae, XVIII – 2s + 1ae, XIX – 2s + 1ae, XX – 2s + 1ae, XXI – 2s + 1ae, XXII – 0s, XXIII – 1s, XXIV – 2s, XXV – 2s, XXVI – 2s, XXVII–XXVIII – 4s + 1ae.

Antenna (Fig. 12A), coxa with 1, basis with 2 setae; endopod segment 1 with 2 setae, segment 2 with 17 setae; exopod 8-segmented, with 1, 3, 1, 1, 1, 1, 1, 3 setae.

Mandible (Fig. 12B, C), gnathobase cutting edge with 8 unequal teeth plus ventral seta; basis with 3 setae; exopodal segments incompletely fused, with 6 setae; first endopod segment with 2 setae, second with 10 setae.

Maxillule (Fig. 12D), praecoxal arthrite with 9 terminal spines, 4 posterior and 1 anterior setae; posterior and anterior surface of praecoxal arthrite with small spinules; coxal endite with 6 setae, coxal epipodite with 8 setae; proximal basal endite with 4 setae, distal basal endite with 5 setae; endopod with 14 setae; exopod with 11 setae.

Maxilla (Fig. 12E), proximal praecoxal endite bearing 3 setae plus attenuation in holotype, 4 setae plus attenuation in paratype, distal praecoxal endite with 3 setae; coxal endites with 3 setae each; coxa with 1 outer seta; proximal basal endite with 3 setae; remaining endopod with 8 setae. All endites except for praecoxal endite with surface spinules.

Maxilliped (Fig. 13A), syncoxa with 1 seta on proximal praecoxal endite, 2 setae on middle endite, and 3 setae on distal praecoxal endite; coxal endite with 3 setae; syncoxa with row of spinules. Basis with 3 distal setae; endopod with 2, 4, 4, 3, 3 + 1, and 4 setae and row of spinules at setae basis on segment 3 and 4.

Legs 1–4 biramous (Fig. 13B–E), with 3-segmented exopods and 3-segmented endopods, except leg 1 endopod 1-segmented and leg 2 endopod 2-segmented. Leg 1–4 coxa with inner surface spinules. Legs 2–4 endopod segments with rows of spinules on posterior surface. Terminal spine on exopod segment 3 finely serrated. Seta and spine formula as in Table 5. Leg 1 (Fig. 13B), basis with medial and

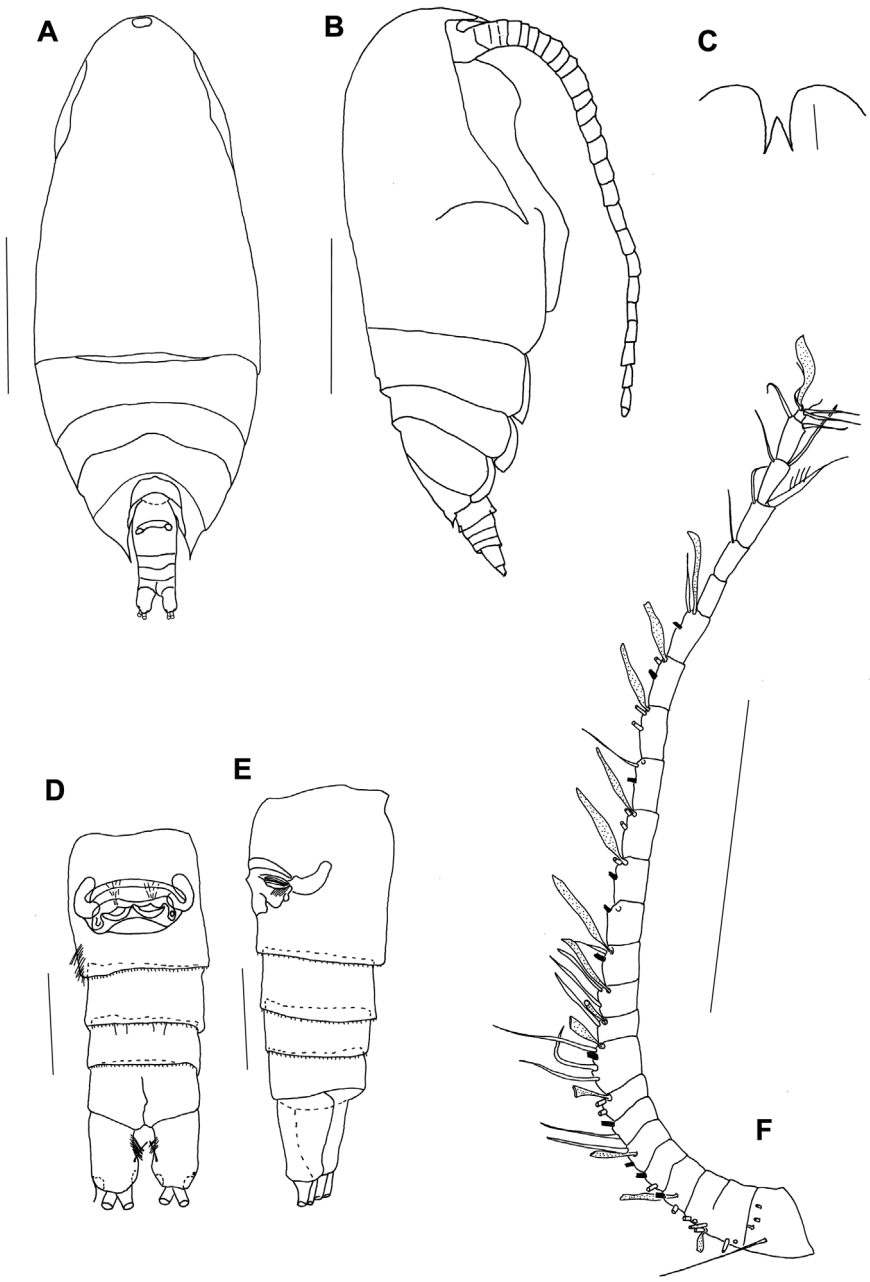

Figure 11. ***Yrocalanus kurilensis*** **sp. nov.**, female, holotype. A, habitus dorsal. B, habitus lateral. C, rostrum ventral. D, urosome ventral. E, urosome lateral. F, antennule, blacked out setae represent a different kind of short setae present on several segments. Scale bars: A–B, F: 0.5 mm. C–E: 0.1 mm.

lateral spinules; endopod lateral lobe poorly developed with spinules; exopod segment 2 with long lateral spine extending to distal end of exopod 3, and medial spinules, segment 3 terminal spine ca. 2.2 times as long as exopod.

Leg 3 (Fig. 13D), exopod segments 1 and 2 with lateral spine (broken in segment 2 in paratype), segment 3 with three lateral spines (1 spine broken in paratype).

Leg 4 (Fig. 13E), coxa with 3 strong distolateral spines and patches of spinules on posterior surface; basis with row of spinules on distal margin.

Adult male: Total length 1.53 and 1.58 mm (Fig. 14A, B). Rostrum (Fig. 14A, C) two-pointed. Cephalosome and pediger 1 almost completely fused (Fig. 14A, B), pedigers 4 and 5 separate. In lateral view posterolateral corners of prosome extended posteriorly into points,

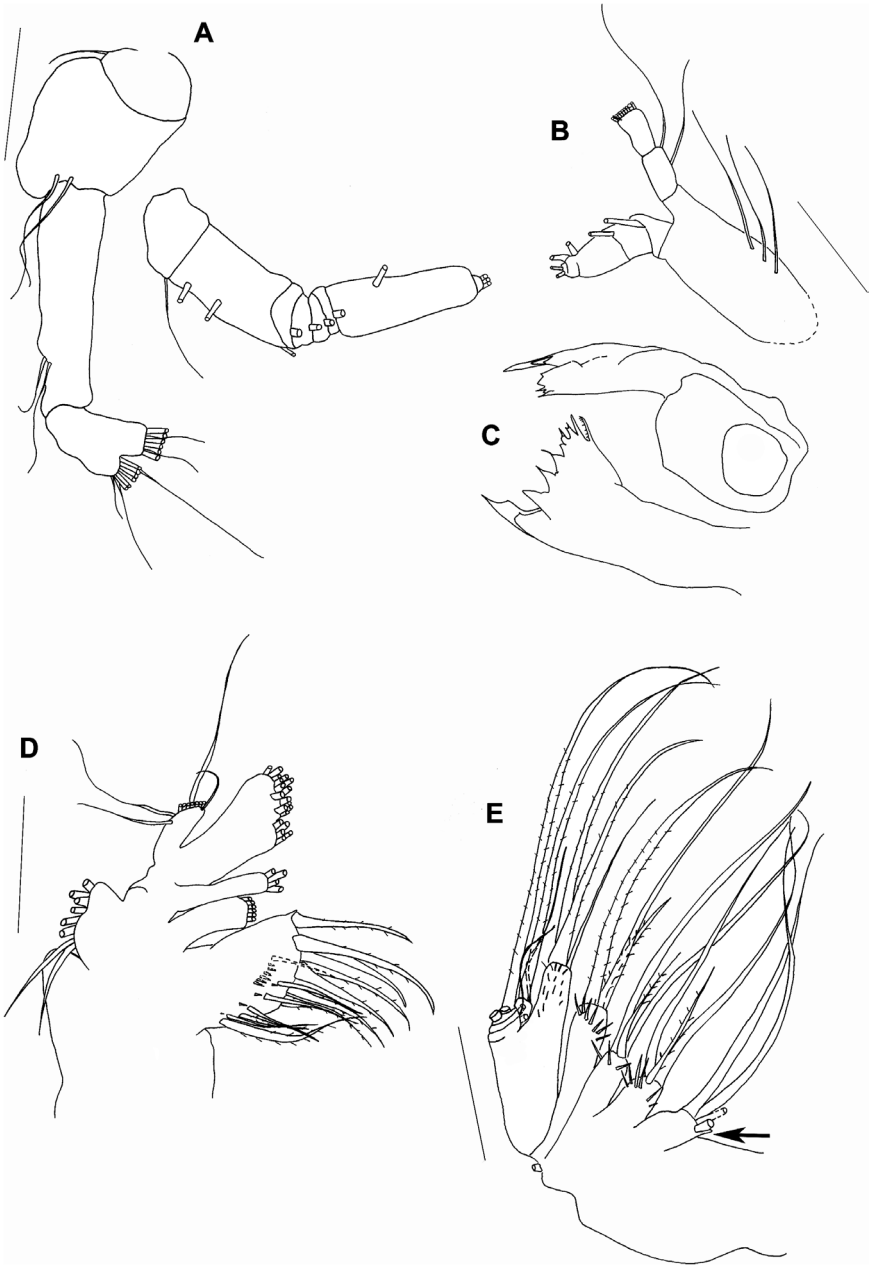

Figure 12. ***Yrocalanus kurilensis*** **sp. nov.**, female, holotype. A, antenna. B–C, mandible with gnathobase figured separately in different positions. D, maxillule. E, maxilla. Scale bars: A–E: 0.1 mm.

slightly extending urosomite 1. Caudal rami (Fig. 14D) symmetrical, with two lateral setae (II and III), three terminal setae (IV–VI) and one dorsal seta (VII)

Left antennule (Fig. 14E) unmodified, of 24 free segments, extending to urosome; armature as follows: I – 1s + 1ae, II–IV – 6s + 4ae, V – 2s + 2ae, VI – 2s + 1ae, VII – 2s + 2ae, VIII – 2s + 1ae, IX – 2s + 2ae, X–XI – 4s + 3ae?, XII – 1s + 1ae; XIII – 2s + 1ae; XIV – 2s + 1ae, XV – 1s + 1ae, XVI – 2s + 1ae, XVII – 2s + 1ae, XVIII – 2s + 1ae, XIX – 2s + 1ae, XX – 2s + 1ae, XXI – 2s + 1ae, XXII – 0s XXIII – 1s + 1ae, XXIV – 2s + 1ae, XXV – 2s + 1ae, XXVI – 2s, XXVII–XXVIII – 3s + 1ae.

Right antennule (Fig. 14F, G) strongly modified for grasping, of 24 free segments; segments XX–XXVI strongly enlarged; segment XX with 1 distal strong hook-like attenuation, segment XXI with a straight, strong, spine-like attenuation and a serrated strong spine, segments XXIII–XXIV with a large plate, segment XXVI with lateral lamella; hinges occurring between segments XVIII and XIX, XIX and XX, XX and

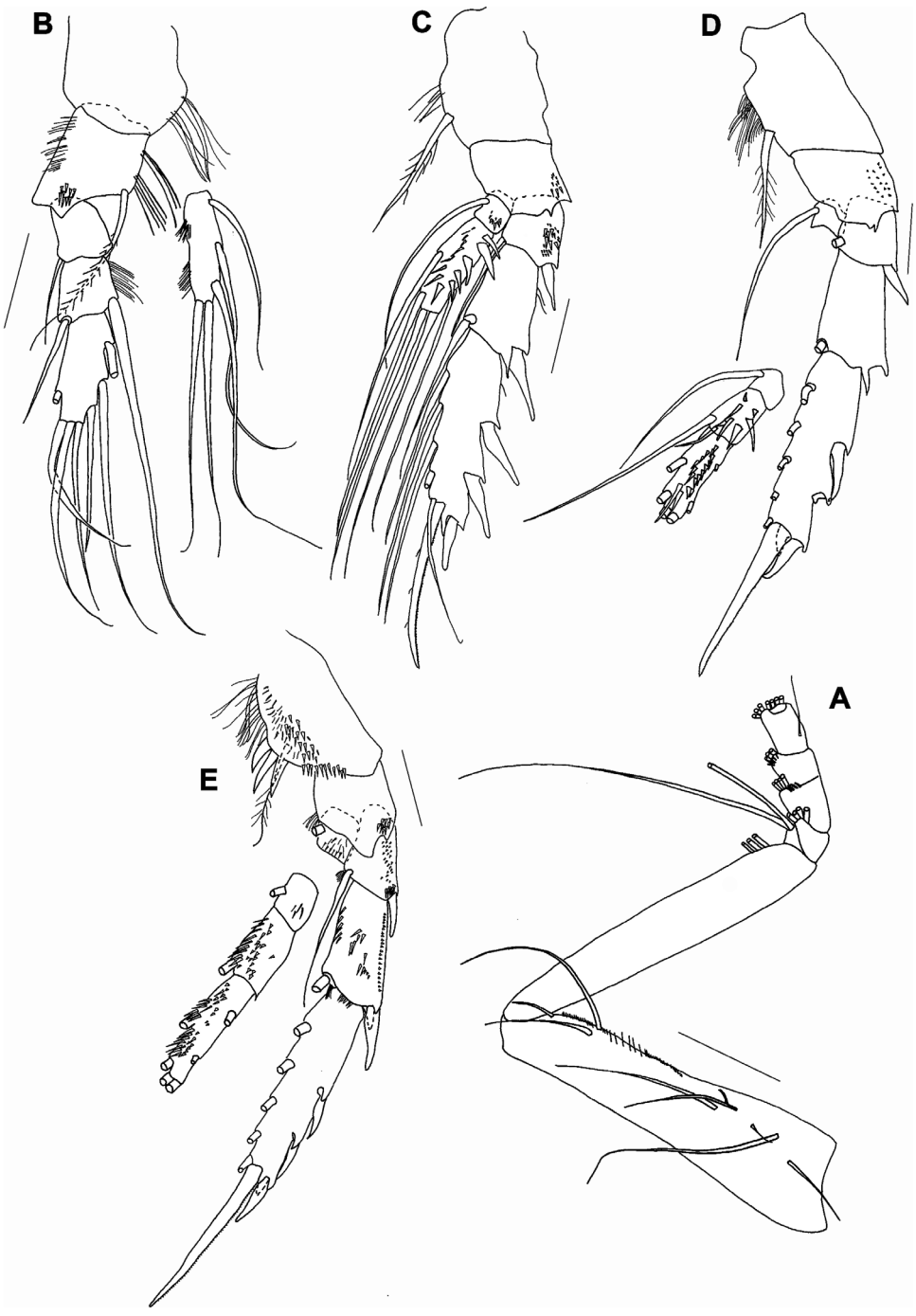

Figure 13. ***Yrocalanus kurilensis*** **sp. nov.**, female, holotype. A, maxilliped. B, leg 1 with endopod figured separately. C, leg 2. D, leg 3 with endopod figured separately. E, leg 4 with endopod figured separately. Scale bars: A–E: 0.1 mm.

XXI, and XXII and XXIII. Armature as follows: I – 1s + 1ae, II to III – 4s + 3ae, IV – 2s + 1ae, segments V-XI armature as in left antennule; XII – 1s + 1ae, XIII-XIX armature as in left antennule, XX – 1s + 1ae + spine like attenuation XXI – 1s + 2 spine like attenuations, XXII – 1s + 1ae, XXIII –XXIV – 2s + 1ae + 1?, XXV – 2s + 1ae, XXVI – 2s, XXVII-XVIII – 4s + 1ae.

Antenna as in female, except endopod segment 2 with 16 setae. Mandible similar to that of female, except basis with 2 setae. Maxillule as in female, but exopod with 10 setae. Maxilla similar to that of

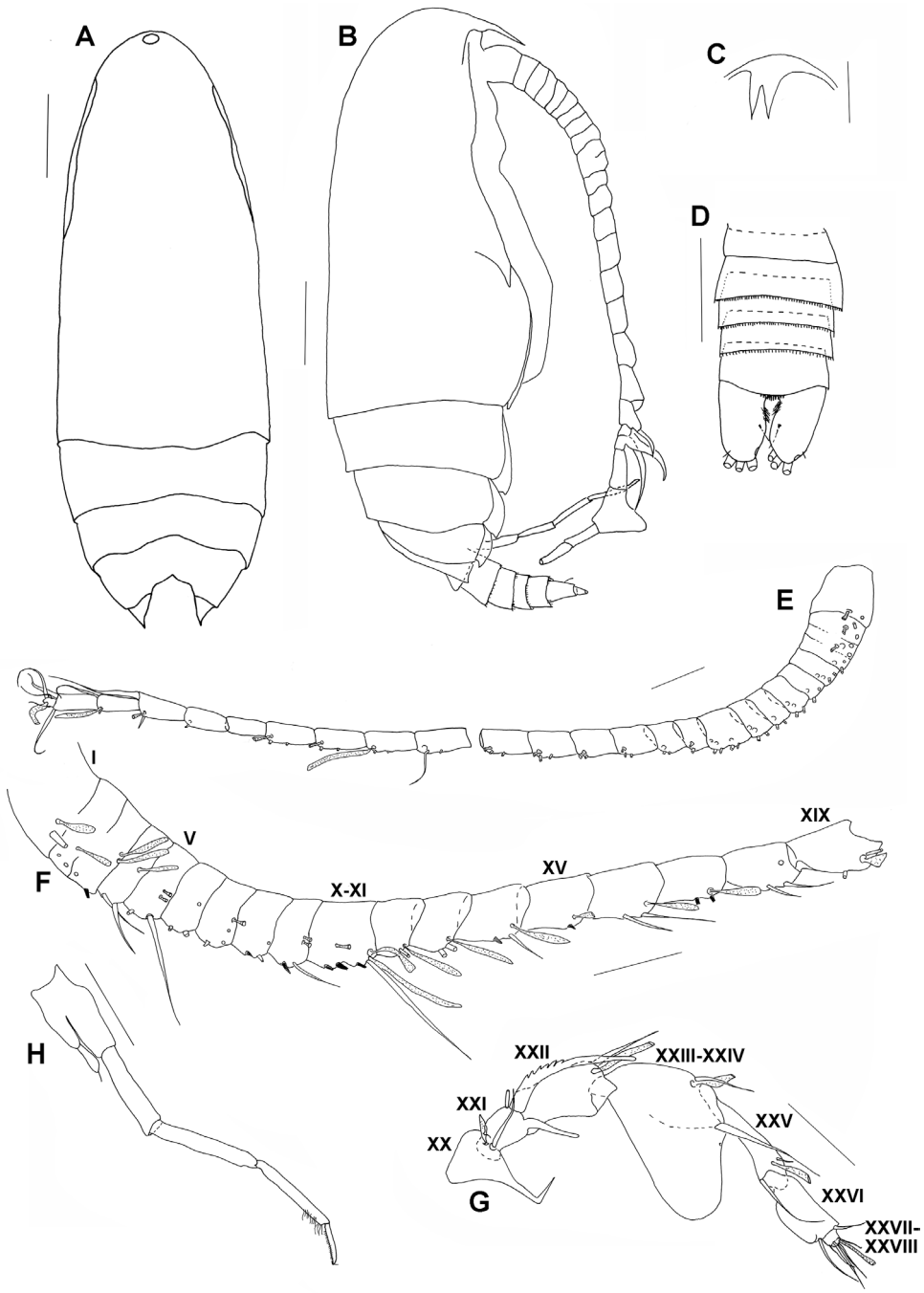

Figure 14. ***Yrocalanus kurilensis*** **sp. nov.**, male, paratype. A, habitus dorsal, urosome not figured. B, habitus lateral. C, rostrum ventral. D, urosome dorsal. E, left antennule. F, right antennule segments I–XIX. G, right antennule, segments XX–XXVIII. H, leg 5. Scale bars: A–B: 0.2 mm. C–H: 0.1 mm.

female, but proximal praecoxal endite bearing 3 setae. Maxilliped as in female.

Segmentation of legs 1–4 as in female. Coxa of leg 4 without strong distolateral spines. Endo- and exopods of leg 4 missing in paratypes. Leg 5 (Fig. 14H) uniramous on both sides. Right leg 2-segmented, with small terminal spine, shorter than left leg. Left leg with 3-segmented exopod. Exopod segment 2 with row of spinules distally, exopod segment 3 with medial row of spinules.

Remarks: The new species shares the main morphological characters with species of the genus

Table 5. Seta and spine formula of ***Yrocalanus kurilensis* sp. nov.** from the Kurile-Kamchatka trench

Leg 1	coxa 0-0	basis 0-1	exp I-0; I-1; 2, 1, 4
			enp 0, 2, 3
Leg 2	coxa 0-1	basis 0-0	exp I-1; I-1; III, I, 5
			enp 0-1; 1, 2, 2
Leg 3	coxa 0-1	basis 0-0	exp I-1; I-1; III, I, 5
			enp 0-1; 0-1; 2, 2, 2
Leg 4	coxa 0-1	basis 0-0	exp I-1; I-1; III, I, 5
			enp 0-1; 0-1; 2, 2, 2

Yrocalanus (Renz *et al.*, 2013). Both sexes are so far only known for *Y. antarcticus* Renz, Markhaseva & Schulz, 2012, while *Y. admirabilis* Andronov, 1992 is only known from a male and *Y. bicornis* and *Y. asymmetricus* Markhaseva & Ferrari, 1996 only from female specimens.

Females of *Yrocalanus kurilensis* sp. nov. are easily distinguished from the remaining species of this genus by the shape of the rostrum, which is wider at its tips than in other *Yrocalanus* species, the shape of the posterolateral corners of the prosome with narrowed points, which is not found in other *Yrocalanus* species, the form of the genital double-somite, which is symmetrical in *Yrocalanus kurilensis* sp. nov, but asymmetrical in *Y. asymmetricus*, *Y. bicornis* (Markhaseva & Ferrari, 1996) and *Y. antarcticus* (Renz *et al.*, 2012) and the 3 robust spines on the coxa of P4 (only 2 in other *Yrocalanus* females). At least two different types of setae could be observed on the antennule, with short, frayed setae occurring on segment V–VIII, XI, XIV–XVI, XVIII and XX–XXI.

Males of *Yrocalanus kurilensis* sp. nov. differ from the remaining species of this genus in the shape of ancestral segments of the right antennule. Segment XXI is equipped with a serrated spine reaching the lower third of compound segment XXIII–XXIV, while it reaches the distal border of segment XXIII–XXIV in *Y. antarcticus* and the distal border of segment XXV in *Y. admirabilis* (Andronov, 1992). Fused segments XXIII–XXIV are equipped with a large plate spanning the whole segment in *Yrocalanus kurilensis* sp. nov. This plate spans only half of the segment in *Y. antarcticus* and has the form of a small bulge in *Y. admirabilis*. Furthemore, the elongated projection on segment XXVI in *Y. antarcticus* and *Y. admirabilis* is absent in *Y. kurilensis* sp. nov. Differences can also be observed in the number and morphology of the spines and segments of leg 5, which is uniramous in *Y. kurilensis* sp. nov, but shows rudimentary endopods in *Y. antarcticus* and *Y. asymmetricus*. With the discovery of the new species, the maximum size of species within the genus has to be corrected from earlier descriptions (Renz *et al.*, 2013), with currently known members ranging between 0.95 mm (*Y. asymmetricus*) and 1.75 mm (*Y. kurilensis* sp. nov.). With *Y. kurilensis* sp. nov. included into the analysis, the definition for the genus is: small copepods (<1.75 mm). The rostrum is bifid. The proximal inner part of the leg 1 endopod is smooth. The female and male left antennule segment XXII is without a seta. The male right antennule is modified for grasping and of highly complex structure, with the main hinge between segment XXII and fused segments XXIII–XXIV. The male P5 is uniramous or indistinctly biramous with small endopodal buds and with the distal exopod segments with or without spines.

Molecular phylogeny

To gain insights into the relationships among the evolutionarily youngest calanoid copepod groups, different species of Ryocalanoidea (genera *Ryocalanus* and *Yrocalanus*) and Spinocalanoidea (genera *Spinocalanus* Giesbrecht, 1888, *Caudacalanus* Markhaseva & Schulz, 2008) from the South Atlantic (Brazilian Basin), North Atlantic (Great Meteor Seamount) and North Pacific (Kurile-Kamchatka trench) were analysed using multi-gene approaches. Sequencing of *Cytb* was successful only for one individual of *Yrocalanus kurilensis* sp. nov. from the Kurile-Kamchatka trench and failed completely for *COI* for this species. Amplification and/or sequencing of *Cytb* was furthermore not successful for three *Ryocalanus* individuals from the South Atlantic, and *Spinocalanus cf. magnus* Wolenden, 1904 and *Paraeuchaeta parvula* (Park, 1978) from the North Atlantic. ITS2 amplification/sequencing did not work for *Spinocalanus abyssalis* Giesbrecht, 1888 and *S. aspinosus* Park, 1970. Sequencing was, however, successful for nuclear genes 18S and 28S (see accession numbers in Table 1 for successfully sequenced genes).

The integration of our data into the sequence dataset of Bradford-Grieve *et al.* (2014) resulted in support for the same calanoid superfamily phylogeny as the original analyses by Blanco-Bercial *et al.* (2011) and Bradford-Grieve *et al.* (2014).

Adding these new data resulted in a well-supported relationship between ryocalanoidean, spinocalanoidean and clausocalanoidean copepods [Bootstrap Support (BS): 87/96, Bayesian Posterior Probability (BPP): 1/1, without and with regard of the three different codon positions for the mitochondrial genes *COI* and *Cytb*, Fig. 15].

Within this clade, Ryocalanoidea and Spinocalanoidea form a highly supported clade (BS: 99/100; BPP: 1/1). The species of Ryocalanidae (*Ryocalanus* and *Yrocalanus*) did not form a monophyletic group, as only species of

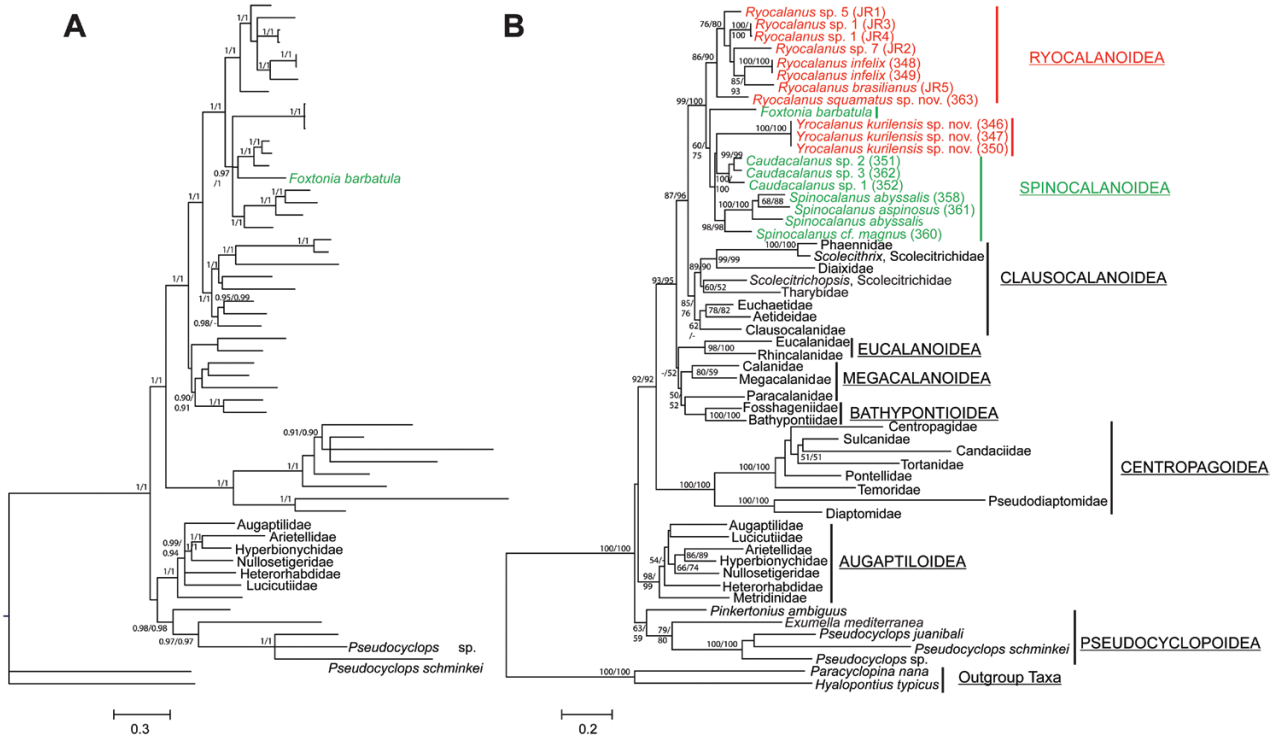

Figure 15. Phylogeny of the Ryocalanoidea (red) and selected representatives from Spinocalanoidea (green) within calanoid superfamilies based on concatenated genes of 18S (931 bp), 28S (733 bp), *COI* (547 bp) and cytochrome *b* (327 bp). New sequences are marked with an ID (e.g. JR3), while the remaining data are used from Bradford-Grieve *et al.* (2014). A, Bayesian Inference with Bayesian posterior probabilities >0.90 are shown. B, Maximum Likelihood analysis with 10 000 bootstrap replicates. Bootstrap values >50 are shown. First numbers without and second number with consideration of codon positions for mitochondrial genes *COI* and cytochrome *b*. The illustrated topology of the tree is from the analysis without consideration of codon positions for *COI* and cytochrome *b*.

Ryocalanus were found in one clade (BS: 86/90; BPP: 1/1), while *Yrocalanus* was located in a supported clade with species of Spinocalanidae (*Spinocalanus*) and Arctokonstantinidae (*Caudacalanus* and *Foxtonia* Hulsemann & Grice, 1963) (BS: 60/75; BPP: 0.97/1).

The Arctoconstantinidae were not supported as a monophyletic group in both analyses. Individuals of the same species (i.e. *Yrocalanus kurilensis* sp. nov. and *Ryocalanus infelix*) and species within the same genera (i.e. *Ryocalanus*, *Spinocalanus* and *Caudacalanus*) were highly supported as close relatives (BS: 100/100; BPP: 1/1, respectively).

The close relationship of Ryocalanidae, Spinocalanidae and Arctokonstantinidae and the position of Ryocalanidae in the system of Calanoida was investigated using longer fragments of 18S, 28S and *COI*, and *Cytb* together with ITS2 (Fig. 16). This analysis revealed a high support of species within the same genus (BS: ≥99/100 and BPP: 1/1, respectively, as well as high support of the close relationship of the superfamilies Ryocalanoidea and Spinocalanoidea (BS: 100/100; BPP: 1/1). Again, Ryocalanidae could not be supported as a monophyletic clade as *Yrocalanus* appeared in a highly supported clade together with all Spinocalanidae and Arctokonstantinidae (BS: 96/94; BPP: 0.95/0.95).

Compared to the multiple-gene analyses, the single-gene analysis of 28S resulted in similar results with high support of a *Ryocalanus* clade and one clade comprising *Spinocalanus*, *Caudacalanus* and *Yrocalanus* (results not shown).

DNA SEQUENCE VARIATION

There was a considerable variation in the rate of molecular evolution between the three gene loci, 18S, 28S and ITS2, with highest interspecific levels of divergence within ITS2 (0.059–0.539) and lowest levels in 18S (0.001–0.029; Table 6). Uncorrected genetic p-distances between the genera *Yrocalanus* and *Ryocalanus* within the Ryocalanoidea were found to be higher (18S: 0.016–0.022; 28S: 0.096–0.12; ITS2: 0.462–0.516) than between the genera *Caudacalanus* and *Spinocalanus* within the Spinocalanoidea (18S: 0.012–0.016; 28S:

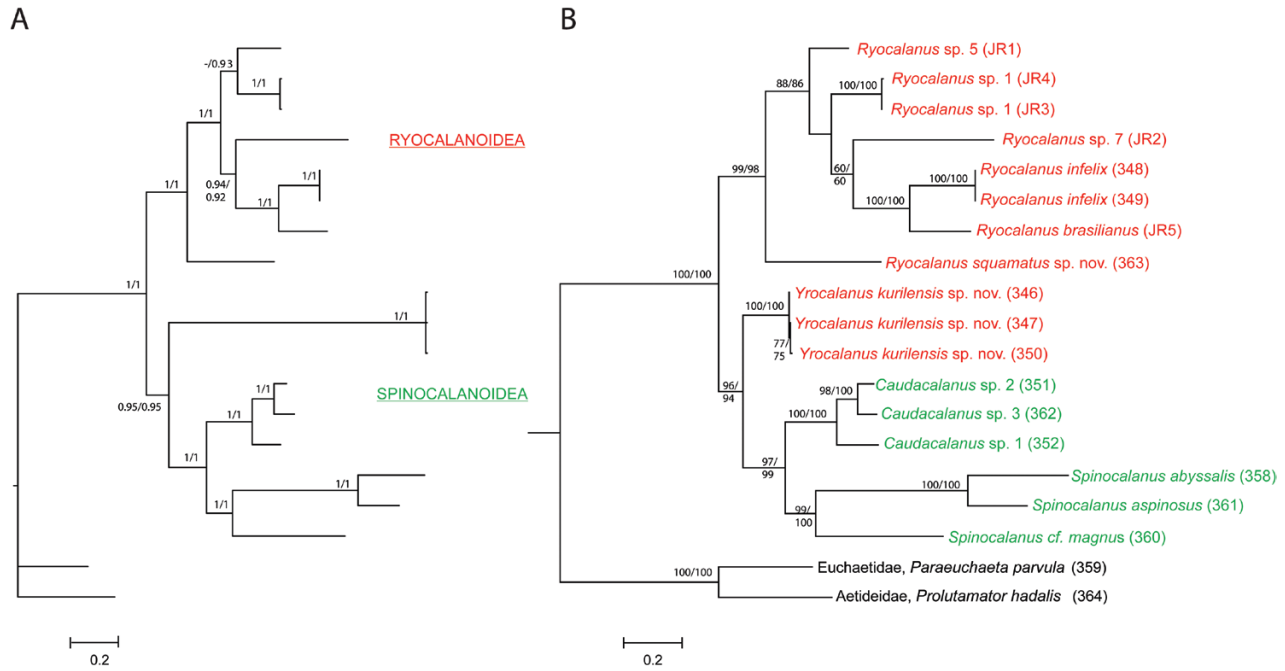

Figure 16. Relationship of the Ryocalanoidea (red) and Spinocalanoidea (green) based on concatenated genes of 18S (1767 bp), 28S (842 bp), ITS2 (266 bp), *COI* (657 bp) and cytochrome *b* (327 bp). A, Bayesian Inference with Bayesian posterior probabilities >0.90 are shown. B, Maximum Likelihood analysis with 10 000 bootstrap replicates. Bootstrap values >50 are shown. First numbers without and second number with consideration of codon positions for mitochondrial genes *COI* and cytochrome *b*. The illustrated topology of the tree is from the analysis without consideration of codon positions for *COI* and cytochrome *b*.

0.056–0.069; ITS2: 0.339–0.368). Highest distances were found between *Spinocalanus* and *Yrocalanus* for 18S, *Yrocalanus* and *Ryocalanus* for 28S and *Spinocalanus* and *Yrocalanus* for ITS2. Within the ribosomal locus 18S, sequence distances were low between *Caudacalanus* and most *Ryocalanus* species compared to differences between species of other genera. Intraspecific genetic divergences for *Yrocalanus kurilensis* sp. nov. and *Ryocalanus infelix* were 0 for 18S and 28S, and 0–0.005 for ITS2.

DISCUSSION

MORPHOLOGICAL EVIDENCE ON THE VALIDITY OF RYOCALANOIDEA

The new copepod species of *Ryocalanus* and *Yrocalanus* found in the Kurile-Kamchatka trench can be attributed to the family Ryocalanidae within the Ryocalanoidea as currently defined based on a particular suite of characteristics. These are the one-segmented endopod of leg 1, the armature of the third expopod segment of leg 1 as II, I, 4 (2 lateral and 1 terminal spine plus 4 medial setae) in combination with the armature of the third exopodal segment of leg 2–4 as III, I, 5, as well as the right antennule in the males, which is strongly modified for grasping. However, the differently formed grasping right antennule in males, with the main hinges between segments XXII/XXIII and XXIV in *Ryocalanus* and between XXII and XXIII/XXIV in *Yrocalanus* clearly separates these genera.

This is the first time the close relationship between Spinocalanoidea and Ryocalanoidea was revealed based on molecular evidence. A monophyly of Ryocalanidae was, however, not supported by molecular multi-gene analyses using different fragment lengths, different partitions and analyses as well as single-gene analysis of 28S rDNA. The differences indicated by morphological and molecular results therefore support the necessity to discuss the relationships of ryocalanoidean and spinocalanoidean copepods.

Compared with ryocalanoidean copepods, Spinocalanoidea are characterized by an armature of I, I, 4 on the third exopod segment of the first leg. Morphologically, this armature clearly separates ryocalanoideans and spinocalanoideans. In a recent publication, Andronov (2014) points out the close relationship between Spinocalanoidea and Ryocalanoidea, based on the structure of the rostrum, the setation of all oral limbs and the structure and segmentation of legs 1–4. The latter includes the rudimentary outer lobe on the leg 1 endopod, the presence of 5 setae at the inner border of legs 2–4 exopod segment 3 as well as 6 setae at the endopod segment 3 of legs 3–4, the absence of leg 5 in females and the very simple structure

Table 6. Uncorrected genetic p-distances for Ryocalanoidea (*Ryocalanus* and *Yrocalanus*) and Spinocalanoidea (*Caudacalanus* and *Spinocalanus*) **A: 18S rDNA**

18S		*Ryocalanus*							*Yrocalanus*			*Caudacalanus*			*Spinocalanus*	
		JR1	JR4	JR3	JR2	348	349	JR5	363	346	347	350	351	352	362	358	360
JR1	*Ryocalanus* sp. 5																
JR4	*Ryocalanus* sp. 1	0.001															
JR3	*Ryocalanus* sp. 1	0.001	0.000														
JR2	*Ryocalanus* sp. 7	0.009	0.010	0.010													
348	*Ryocalanus infelix*	0.002	0.000	0.002	0.009												
349	*Ryocalanus infelix*	0.002	0.002	0.002	0.009	0.000											
JR5	*Ryocalanus brasilianus*	0.004	0.003	0.003	0.011	0.002	0.002										
363	*Ryocalanus squamatus* sp. nov.	0.002	0.002	0.002	0.011	0.004	0.004	0.006									
346	*Yrocalanus kurilensis* sp. nov.	0.016	0.017	0.017	0.022	0.018	0.018	0.021	0.016								
347	*Yrocalanus kurilensis* sp. nov.	0.016	0.017	0.017	0.022	0.018	0.018	0.021	0.016	0.000							
350	*Yrocalanus kurilensis* sp. nov.	0.016	0.017	0.017	0.022	0.018	0.018	0.021	0.016	0.000	0.000						
351	*Caudacalanus* sp. 2	0.002	0.003	0.003	0.011	0.004	0.004	0.006	0.002	0.015	0.015	0.015					
352	*Caudacalanus* sp. 1	0.003	0.003	0.003	0.012	0.005	0.005	0.007	0.002	0.016	0.016	0.016	0.001				
362	*Caudacalanus* sp. 3	0.003	0.003	0.003	0.012	0.005	0.005	0.007	0.002	0.016	0.016	0.016	0.001	0.001			
358	*Spinocalanus abyssalis*	0.013	0.012	0.012	0.022	0.014	0.014	0.015	0.014	0.027	0.027	0.027	0.014	0.015	0.015		
360	*Spinocalanus* cf. *magnus*	0.015	0.014	0.014	0.022	0.015	0.015	0.017	0.015	0.029	0.029	0.029	0.016	0.016	0.016	0.022	
361	*Spinocalanus aspinosus*	0.012	0.012	0.012	0.022	0.013	0.013	0.014	0.013	0.026	0.026	0.026	0.012	0.013	0.013	0.002	0.022

B: 28S rDNA

28S		*Ryocalanus*							*Yrocalanus*			*Caudacalanus*			*Spinocalanus*	
		JR1	JR4	JR3	JR2	348	349	JR5	363	346	347	350	351	352	362	358	360
JR1	*Ryocalanus* sp. 5																
JR4	*Ryocalanus* sp. 1	0.035															
JR3	*Ryocalanus* sp. 1	0.036	0.001														
JR2	*Ryocalanus* sp. 7	0.060	0.064	0.063													
348	*Ryocalanus infelix*	0.049	0.050	0.051	0.070												
349	*Ryocalanus infelix*	0.049	0.050	0.051	0.070	0.000											
JR5	*Ryocalanus brasilianus*	0.053	0.050	0.000	0.069	0.025	0.025										
363	*Ryocalanus squamatus* sp. nov.	0.053	0.053	0.052	0.083	0.063	0.063	0.066									
346	*Yrocalanus kurilensis* sp. nov.	0.096	0.107	0.105	0.120	0.101	0.101	0.096	0.105								
347	*Yrocalanus kurilensis* sp. nov.	0.096	0.107	0.105	0.120	0.101	0.101	0.096	0.105	0.000							
350	*Yrocalanus kurilensis* sp. nov.	0.096	0.107	0.105	0.119	0.101	0.101	0.095	0.105	0.000	0.000						
351	*Caudacalanus* sp. 2	0.074	0.086	0.085	0.106	0.072	0.072	0.086	0.079	0.092	0.092	0.092					
352	*Caudacalanus* sp. 1	0.081	0.084	0.083	0.113	0.079	0.079	0.093	0.073	0.101	0.101	0.101	0.027				
362	*Caudacalanus* sp. 3	0.080	0.089	0.088	0.112	0.076	0.076	0.093	0.077	0.100	0.100	0.100	0.010	0.019			
358	*Spinocalanus abyssalis*	0.094	0.091	0.090	0.111	0.090	0.090	0.104	0.074	0.116	0.116	0.116	0.066	0.064	0.069		
360	*Spinocalanus* cf. *magnus*	0.085	0.087	0.086	0.104	0.082	0.082	0.091	0.069	0.100	0.100	0.100	0.061	0.058	0.056	0.059	
361	*Spinocalanus aspinosus*	0.091	0.088	0.088	0.106	0.091	0.091	0.104	0.072	0.111	0.111	0.111	0.065	0.063	0.068	0.008	0.058

C: ITS2

ITS2		*Ryocalanus*							*Yrocalanus*			*Caudacalanus*			*Spinocalanus*	
		JR1	JR4	JR3	JR2	348	349	JR5	363	346	347	350	351	352	362	358	360
JR1	*Ryocalanus* sp. 5																
JR4	*Ryocalanus* sp. 1	0.178															
JR3	*Ryocalanus* sp. 1	0.178	0.000														
JR2	*Ryocalanus* sp. 7	0.289	0.293	0.293													
348	*Ryocalanus infelix*	0.269	0.291	0.291	0.335												
349	*Ryocalanus infelix*	0.269	0.291	0.291	0.335	0.000											
JR5	*Ryocalanus brasilianus*	0.310	0.276	0.276	0.349	0.103	0.103										
363	*Ryocalanus squamatus* sp. nov.	0.308	0.338	0.338	0.312	0.340	0.340	0.353									
346	*Yrocalanus kurilensis* sp. nov.	0.516	0.513	0.513	0.513	0.462	0.462	0.474	0.500								
347	*Yrocalanus kurilensis* sp. nov.	0.516	0.513	0.513	0.513	0.462	0.462	0.474	0.500	0.005							
350	*Yrocalanus kurilensis* sp. nov.	0.516	0.513	0.513	0.513	0.462	0.462	0.474	0.500	0.005	0.005						
351	*Caudacalanus* sp. 2	0.487	0.487	0.487	0.448	0.451	0.451	0.448	0.466	0.516	0.516	0.516					
352	*Caudacalanus* sp. 1	0.469	0.471	0.471	0.458	0.430	0.430	0.443	0.442	0.539	0.539	0.539	0.220				
362	*Caudacalanus* sp. 3	0.497	0.474	0.474	0.445	0.435	0.435	0.438	0.466	0.516	0.516	0.516	0.059	0.220			
358	*Spinocalanus abyssalis*	n/a	n/a	n/a	n/a	n/a	n/a	n/a	n/a	n/a	n/a	n/a	n/a	n/a	n/a		
360	*Spinocalanus* cf. *magnus*	0.438	0.438	0.432	0.466	0.428	0.428	0.453	0.442	0.471	0.471	0.471	0.368	0.339	0.357	n/a	
361	*Spinocalanus aspinosus*	n/a	n/a	n/a	n/a	n/a	n/a	n/a	n/a	n/a	n/a	n/a	n/a	n/a	n/a	n/a	n/a

of the male leg 5. Andronov (2014) considered all these characters to be typical of the representatives of the Spinocalanidae. Restructuring the classification system for calanoid copepods Andronov remarked that the grasping right antennule in males is the only character truly distinguishing ryocalanid from spinocalanid copepods. He proposed to lower the status of Ryocalanoidea to Ryocalaninae and place them into the family Spinocalanidae.

While the new hypothesis by Andronov (2014) has not been discussed in the recent literature so far, some other morphological evidence supports a close relationship between ryocalanid and spinocalanid individuals. In at least two members of the family Ryocalanidae (*Y. asymmetricus* and *Y. bicornis*) that were re-examined for this study, the armature of the third exopod of the first leg was found to be I, I, 4, as described by Markhaseva & Ferrari (1996). Additionally, while spinocalanoidean copepods are considered to lack any geniculation or hinges of the male right antennule, the males of many spinocalanoidean species have an asymmetrical antennule with fusions, e.g. between segments XXII–XXIII on the right side, and differences in the form of the segments (e.g. Bradford, 1994; Boxshall & Halsey 2004; Ivanenko *et al.*, 2007). However, this fusion of segments was only observed in *Ryocalanus*.

Phylogenetic position of the Ryocalanidae and Ryocalanoidea in the order Calanoida

Molecular approaches are suitable for species assignment and species descriptions but also help to gain insights into the evolutionary history of calanoids, when nuclear 18S rDNA, 28S rDNA and internal transcribed spacer 2 (ITS2) are considered (e.g. Braga *et al.*, 1999; Bucklin *et al.*, 2003), because these markers are more informative for phylogenetic analyses at intergeneric and higher taxonomic levels.

Among the Ryocalanoidea, *Ryocalanus squamatus* sp. nov. was separated from a clade containing all other *Ryocalanus* species. From a morphological perspective, *R. squamatus* sp. nov. differed from all other *Ryocalanus* species by the form of the rostrum, an only slightly asymmetrical genital somite, the spinulation of pedigers 2–5, as well as the anterior part of swimming legs, the lack of strong spines on the coxa of P4, the antennule, being covered by scale-like structures, as well as the morphology and setation of some oral limbs. Together with the molecular evidence, some of these differences in setation and habitus characteristics might point towards a new genus of ryocalanid copepods related to *Ryocalanus*. Furthermore, our molecular analyses confirmed the status of the *Ryocalanus infelix* female, which was so far unknown.

Within the Spinocalanoidea, the family Spinocalanidae was supported in a clade that was separated from *Yrocalanus* and species belonging to the Arctokonstantinidae. The latter family was established by Markhaseva & Kosobokova (2001) and later treated as a synonym for Spinocalanidae by Boxshall & Halsey (2004). Markhaseva (2008) and Markhaseva & Schulz (2008) gave a detailed analysis of the Arctokonstantinidae, concluding that, based on several apomorphies, this family represents a monophyletic group. The multi-gene analyses presented here did, however, not support a clade comprising *Caudacalanus* and *Foxtonia*. While *Foxtonia* is a pelagic deep-water inhabitant, species of *Caudacalanus* are exclusively found in benthopelagic waters and both genera are so far only known from few female individuals. The discovery of males will, therefore, be crucial to clarify the relationship between these genera.

Our multi-gene analysis was based on the dataset for calanoid superfamilies compiled by Bradford-Grieve *et al.* (2014) and Blanco-Bercial *et al.* (2011). Addition of the previously missing Ryocalanoidea and extra members of the Spinocalanoidea expanded the dataset used by these authors and enabled us to focus our investigations on relationships among the youngest lineages within the Calanoida. Sequences of the nuclear ITS2, a region between the 5.8S and 28S nuclear rDNA, were added. This region is known to show higher resolution below subfamily level in Veneridae (Bivalvia; Salvi & Mariottini, 2012), is generally more conserved than *COI* and likely to be subject to different selective pressures (Marinucci *et al.*, 1999).

The retrieval of most superfamilies in the previous molecular multi-gene analyses by Blanco-Bercial *et al.* (2011) and Bradford-Grieve *et al.* (2014) served as a solid database that is, with few exceptions, largely in accordance with earlier morphological analysis of calanoids (Andronov, 1974; Park, 1986; Boxshall & Halsey, 2004) and, most recently, a cladistic analysis by Bradford-Grieve *et al.* (2010). Here, we accept the modified system as presented in Bradford-Grieve *et al.* (2014). The inclusion of *Ryocalanus*, *Yrocalanus* and typical benthopelagic Spinocalanoidea (*Caudacalanus*) in the dataset did not change the topology of the tree, whether each family was represented by a single individual, as in previous analyses (results not shown), or whether families were represented by all species analysed here.

Earlier molecular multi-gene analyses (Blanco-Bercial *et al.*, 2011; Bradford-Grieve *et al.*, 2014) already pointed out the close relationship between Spinocalanoidea and Clausocalanoidea. Molecular multi-gene analyses now revealed the close relationship between the youngest calanoid superfamilies Clausocalanoidea, Spinocalanoidea and Ryocalanoidea, with the latter two forming a highly supported clade reflecting their close relationship.

However, the analyses did not result in support for the monophyly of Ryocalanoidea. *Yrocalanus* (here represented by three individuals from *Y. kurilensis* sp. nov.) showed a closer relationship to spinocalanoidean species (*Spinocalanus* and *Caudacalanus*) than to *Ryocalanus*, as indicated by a highly supported clade. These results contrast with the close relationship of Ryocalanoidea based on morphological data. While the results based on molecular data might indicate a close connection between ryocalanoidean and spinocalanoidean taxa, some methodological reasons could also cause the lacking retrieval of the monophyletic relationship. Since Ryocalanoidea and Spinocalanoidea are the evolutionary most recently diverged lineages together with Clausocalanoidea (Park, 1986), the selected genes may not be able to resolve their phylogeny. Independently evolving morphological and molecular characters (e.g. Bucklin & Frost, 2009; Thum & Harrison, 2009) were earlier pointed out to be one reason for differences in phylogenetic analysis based on molecular and morphological data. Furthermore, molecular multi-gene analyses, including four different genes, are currently only available for one genus of Spinocalanidae (*Spinocalanus*). The polyphyletic relationship found in a study based on *COI* and 18S for Spinocalanidae by Bode *et al.* (2017) was, among other factors, attributed to the lack of a wide coverage of genera within the analysis, as it differed from the phylogenetic hypotheses of the Spinocalanidae based on morphological characters (Fleminger, 1983; Schulz, 1989).

Interspecific sequence divergences were in the range of divergences observed within other taxa of Calanoida for the more conserved regions 18S (Bucklin *et al.*, 2003; Blanco-Bercial *et al.*, 2011; Bode *et al.*, 2017) and 28S (Blanco-Bercial *et al.*, 2011). However, they were high for the less conserved region ITS2 compared to differences within, e.g. *Clausocalanus* Giesbrecht, 1888 (Bucklin & Frost, 2009). We speculate that a fast, adaptive radiation into the benthopelagic environment has occurred, which shows high calanoid diversity comparable to several other pelagic habitats (Renz & Markhaseva, 2015) and probably supports speciation by providing a high degree of niche availability, as also suggested for deep sea amphipods (Corrigan *et al.*, 2013). The resulting large molecular divergences between closely related taxa could be the reason for the failure to resolve the true relationship between and within Spinocalanoidea and Ryocalanoidea.

We conclude that an unambiguous interpretation of the status of Ryocalanoidea within the Calanoida is currently not possible and the morphological and molecular taxonomic approaches lead to different results. Multi-gene analyses do not resolve and support the monophyly of each of the two superfamilies Ryocalanoidea and Spinocalanoidea. This might either be caused by a previously unrecognized close morphological relationship between these taxa or by methodological impediments in our molecular analysis. From the currently known 14 spinocalanoidean genera, only seven are known from females and males, while males for seven genera have yet to be discovered. The morphology of the male antennule seems to be very important for any interpretation of relationships between different genera within the currently accepted ryocalanoidean and spinocalanoidean calanoids. Despite the ambiguous results, we therefore propose to keep the currently accepted system until further data on the male antennule morphology and molecular data of more genera are available.

ACKNOWLEDGEMENTS

The authors thank Professor Pedro Martinez Arbizu and Professor Angelika Brandt, who provided the material for this study and Karen Jeskulke, who assisted during lab work for genetic analysis. Special thanks go to Dr Leocadio Blanco-Bercial for providing sequence alignments of data analysed during their study and support in the phylogenetic analysis. The authors acknowledge valuable comments by Dr Janet Bradford-Grieve and two anonymous reviewers. This study was funded by the Federal Ministry of Education and Research of Germany (BMBF Grant No. 03F0499A and 03F0664A) and the Land Niedersachsen and is part of the DFG initiative 'Taxonomics' (RE 2808/3-1) and the ZIN theme (52) AAAAA-A17-117030310207-3. Elena Markhaseva acknowledges support by a stipendium from the Research Institute Senckenberg. This is publication number 57 from the Senckenberg am Meer Metabarcoding and Molecular Laboratory.

REFERENCES

Aarbakke ONS, Bucklin A, Halsband C, Norrbin F. 2014. Comparative phylogeography and demographic history of five sibling species of *Pseudocalanus* (Copepoda: Calanoida) in the North Atlantic Ocean. *Journal of Experimental Marine Biology and Ecology* **461:** 479–488.

Altekar G, Dwarkadas S, Huelsenbeck JP, Ronquist F. 2004. Parallel Metropolis coupled Markov chain Monte Carlo for Bayesian phylogenetic inference. *Bioinformatics (Oxford, England)* **20:** 407–415.

Andronov VN. 1974. Phylogenetic relations of large taxa within the suborder Calanoida (Crustacea, Copepoda). *Zoologicheskii Zhurnal* **53:** 1002–1012.

Andronov VN. 1992. *Ryocalanus admirabilis* sp. n. (Copepoda, Calanoida, Ryocalanidae) from the central-eastern Atlantic. *Zoologicheskii Zhurnal* **71:** 140–144 [in Russian].

Andronov VN. 2014. *Phylogeny and revision of calanoid copepods system*. Kaliningrad: Smartbooks, 204 p. [in Russian with English summary].

Blanco-Bercial L, Bradford-Grieve J, Bucklin A. 2011. Molecular phylogeny of the Calanoida (Crustacea: Copepoda). *Molecular Phylogenetics and Evolution* **59:** 103–113.

Bode M, Laakmann S, Kaiser P, Hagen W, Auel H, Cornils A. 2017. Unravelling diversity of deep-sea copepods using integrated morphological and molecular techniques. *Journal of Plankton Research* **39:** 600–617.

Bowman TE, Abele LG. 1982. Classification of the recent Crustacea. In: Abele LG, ed., *The biology of Crustacea, Vol 1. Systematics, the fossil record, and biogeography*. New York: Academic Press, 1–27.

Boxshall GA, Halsey SH. 2004. *An introduction to copepod diversity*. London: The Ray Society.

Bradford-Grieve JM. 1994. The marine fauna of New Zealand: pelagic calanoid Copepoda: Megacalanidae, Calanidae, Paracalanidae, Mecynoceridae, Eucalanidae, Spinocalanidae, Clausocalanidae. *New Zealand Oceanographic Institute memoirs* **102:** 5–156.

Bradford-Grieve JM, Blanco-Bercial L, Boxshall GA. 2017. Revision of family Megacalanidae (Copepoda: Calanoida). *Zootaxa* **4229:** 1–183

Bradford-Grieve JM, Boxshall GA, Ahyong ST, Ohtsuka S. 2010. Cladistic analysis of the calanoid Copepoda. *Invertebrate Systematics* **24:** 291–321.

Bradford-Grieve JM, Boxshall GA, Blanco-Bercial L. 2014. Revision of basal calanoid copepod families, with a description of a new species and genus of Pseudocyclopidae. *Zoological Journal of the Linnean Society* **171:** 507–533.

Braga E, Zardoya R, Meyer A, Yen J. 1999. Mitochondrial and nuclear rRNA based copepod phylogeny with emphasis on the Euchaetidae (Calanoida). *Marine Biology* **133:** 79–90.

Brandt A, Barthel D. 1995. An improved supra- and epibenthic sledge for catching Peracarida (Crustacea, Malacostraca). *Ophelia* **43:** 15–23.

Brenke N. 2005. An epibenthic sledge for operations on marine soft bottom and bedrock. *Marine Technology Society Journal* **39:** 10–19.

Bucklin A, Frost BW. 2009. Morphological and molecular phylogenetic analysis of evolutionary lineages within Clausocalanus (Copepoda: Calanoida). *Journal of Crustacean Biology* **29:** 111–120.

Bucklin A, Frost B, Bradford-Grieve J, Allen L, Copley N. 2003. Molecular systematic and phylogenetic assessment of 34 calanoid copepod species of the Calanidae and Clausocalanidae. *Marine Biology* **142:** 333–343.

Cornils A, Blanco-Bercial L. 2013. Phylogeny of the Paracalanidae Giesbrecht, 1888 (Crustacea: Copepoda: Calanoida). *Molecular Phylogenetics and Evolution* **69:** 861–872.

Edgar RC. 2004. MUSCLE: multiple sequence alignment with high accuracy and high throughput. *Nucleic Acids Research* **32:** 1792–1797.

Corrigan LJ, Horton T, Fotherby H, White TA, Hoelzel AR. 2014. Adaptive evolution of deep-sea amphipods from the superfamily Lysiassanoidea in the North Atlantic. *Evolutionary Biology* **41:** 154–165.

Eyun SI, Lee YH, Suh HL, Kim S, Soh HY. 2007. Genetic identification and molecular phylogeny of *Pseudodiaptomus* species (Calanoida, Pseudodiaptomidae) in Korean waters. *Zoological Science* **24:** 265–271.

Fleminger A. 1983. Description and phylogeny of *Isaacsicalanus paucisetus*, n. gen., n. sp., (Copepoda: Calanoida: Spinocalanidae) from an east Pacific hydrothermal vent site (21°N). *Proceedings of the Biological Society of Washington* **96:** 605–622.

Fleminger A. 1985. Dimorphism and possible sex change in copepods of the family Calanidae. *Marine Biology* **88:** 273–294.

Fosshagen A. 1967. Two new species of calanoid copepods from Norwegian fjords. *Sarsia* **29:** 307–320.

Gelman A, Rubin DB. 1992. Inference from iterative simulation using multiple sequences. *Statistical Science* **7:** 457–472.

Goetze E. 2003. Cryptic speciation on the high seas; global phylogenetics of the copepod family Eucalanidae. *Proceedings of the Royal Society of London B: Biological Sciences* **270:** 2321–2331.

Guindon S, Dufayard JF, Lefort V, Anisimova M, Hordijk W, Gascuel O. 2010. New algorithms and methods to estimate maximum-likelihood phylogenies: assessing the performance of PhyML 3.0. *Systematic Biology* **59:** 307–321.

Hulsemann K, Grice GD. 1963. A new genus and species of bathypelagic calanoid copepod from the North Atlantic. *Deep Sea Research and Oceanographic Abstracts* **10:** 729–733.

Huys R, Boxshall GA. 1991. *Copepod evolution, Vol. 159*. London: The Ray Society.

Ivanenko VN, Defaye D, Cuoc C. 2007. A new calanoid copepod (Spinocalanidae) swarming at a cold seep site on the Gabon continental margin (Southeast Atlantic). *Cahiers de Biologie Marine* **48:** 37–54.

Katoh K, Standley DM. 2013. MAFFT Multiple Sequence Alignment Software Version 7: improvements in performance and usability. *Molecular Biology and Evolution* **30:** 772–780.

Kearse M, Moir R, Wilson A, Stones-Havas S, Cheung M, Sturrock S, Buxton S, Cooper A, Markowitz S, Duran C, Thierer T, Ashton B, Meintjes P, Drummond A. 2012. Geneious Basic: an integrated and extendable desktop software platform for the organization and analysis of sequence data. *Bioinformatics (Oxford, England)* **28:** 1647–1649.

Laakmann S, Gerdts G, Erler R, Knebelsberger T, Martínez Arbizu P, Raupach MJ. 2013. Comparison of molecular species identification for North Sea calanoid copepods (Crustacea) using proteome fingerprints and DNA sequences. *Molecular Ecology Resources* **13:** 862–876.

Laakmann S, Auel H, Kochzius M. 2012. Evolution in the deep sea: biological traits, ecology and phylogenetics of pelagic copepods. *Molecular Phylogenetics and Evolution* **65:** 535–546.

Lanfear R, Calcott B, Ho SY, Guindon S. 2012. Partitionfinder: combined selection of partitioning schemes and substitution models for phylogenetic analyses. *Molecular Biology and Evolution* **29:** 1695–1701.

Lanfear R, Frandsen PB, Wright AM, Senfeld T, Calcott B. 2017. PartitionFinder 2: new methods for selecting partitioned models of evolution for molecular and morphological

phylogenetic analyses. *Molecular Biology and Evolution*. **34:** 772–773. DOI: dx.doi.org/10.1093/molbev/msw260

Marinucci M, Romi R, Mancini P, Di Luca M, Severini C. 1999. Phylogenetic relationships of seven Palearctic members of the maculipennis complex inferred from ITS2 sequence analysis. *Insect Molecular Biology* **8:** 469–480.

Markhaseva EL. 2008. *Foxtosognus rarus* gen. n., sp. n. – a new genus and species of copepods (Copepoda: Calanoida) from the abyssopelagic zone of the Kuril-Kamchatka Trench. *Russian Journal of Marine Biology* **34:** 9–16.

Markhaseva EL, Ferrari FD. 1996. Three new species of *Ryocalanus* from the eastern tropical Pacific (Crustacea, Copepoda: Ryocalanidae). *Zoosystematica Rossica* **4:** 63–70.

Markhaseva EL, Kosobokova K. 2001. *Arctokonstantinus hardingi* (Copepoda, Calanoida, Arctokonstantinidae): new family, new genus, and new species from the bathypelagial Arctic Basin. *Sarsia* **86:** 319–324.

Markhaseva EL, Schulz K. 2008. *Caudacalanus* (Copepoda, Calanoida): a new benthopelagic genus from the abyss of the tropical South Atlantic and Southern Ocean. *Zootaxa* **1866:** 277–289.

Merritt TJ, Shi L, Chase MC, Rex MA, Etter RJ, Quattro JM. 1998. Universal cytochrome b primers facilitate intraspecific studies in molluscan taxa. *Molecular Marine Biology and Biotechnology* **7:** 7–11.

Milligan PJ, Stahl EA, Schizas NV, Turner JT. 2011. Phylogeography of the copepod *Acartia hudsonica* in estuaries of the northeastern United States. *Hydrobiologia* **666:** 155–165.

Ohtsuka S, Huys R. 2001. Sexual dimorphism in calanoid copepods: morphology and function. *Hydrobiologia* **453:** 441–466.

Ohtsuka S, Nishida S. 2017. Copepod biodiversity in Japan: recent advances in Japanese copepodology. In: Motokawa M, Kajihara H, eds. *Species Diversity of Animals in Japan*. Tokyo: Springer, 565–602.

Ohtsuka S, Soh HY, Nishida S. 1997. Evolutionary switching from suspension feeding to carnivory in the calanoid family Heterorhabdidae (Copepoda). *Journal of Crustacean Biology* **17:** 577–595.

Ortman BD. 2008. *DNA barcoding the Medusozoa and Ctenophora*. Storrs: University of Connecticut, 121.

Park T. 1986. Phylogeny of calanoid copepods. *Syllogeus* **58:** 191–196.

Provan J, Beatty GE, Keating SL, Maggs CA, Savidge G. 2009. High dispersal potential has maintained long-term population stability in the North Atlantic copepod *Calanus finmarchicus*. *Proceedings of the Royal Society of London B: Biological Sciences* **276:** 301–307.

Questel JM, Blanco-Bercial L, Hopcroft RR, Bucklin A. 2016. Phylogeography and connectivity of the *Pseudocalanus* (Copepoda: Calanoida) species complex in the eastern North Pacific and the Pacific Arctic Region. *Journal of Plankton Research* **38:** 610–623.

Rambaut A, Suchard MA, Xie D, Drummond AJ. 2014. Tracer v.1.6. Available at: http://beast.bio.ed.ac.uk/Tracer (accessed October 16, 2018).

Renz J, Markhaseva EL. 2015. First insights into genus level diversity and biogeography of deep sea benthopelagic calanoid copepods in the South Atlantic and Southern Ocean. *Deep Sea Research Part I* **105:** 96–110.

Renz J, Markhaseva EL, Schulz K. 2012. *Ryocalanus antarcticus* sp. nov. (Crustacea: Copepoda) – first ryocalanoid from the southern Ocean. *Proceedings of the Zoological Institute RAS* **316:** 148–158.

Renz J, Markhaseva EL, Schulz K. 2013. *Ryocalanus brasilianus* sp. nov. (Crustacea: Copepoda, Calanoida), a new ryocalanoid from the South Atlantic and the segregation of *Yrocalanus* gen. nov. *Zoosystematics and Evolution* **89:** 247–258.

Ronquist F, Huelsenbeck J, Teslenko M. 2011. *MrBayes version 3.2 manual: tutorials and model summaries*. Distributed with the software from http://brahms.biology.rochester.edu/software.html

Ronquist F, Teslenko M, van der Mark P, Ayres DL, Darling A, Höhna S, Larget B, Liu L, Suchard MA, Huelsenbeck JP. 2012. MrBayes 3.2: efficient Bayesian phylogenetic inference and model choice across a large model space. *Systematic Biology* **61:** 539–542.

Salvi D, Mariottini P. 2012. Molecular phylogenetics in 2D: ITS2 rRNA evolution and sequence-structure barcode from Veneridae to Bivalvia. *Molecular Phylogenetics and Evolution* **65:** 792–798.

Schulz, K. 1989. Notes on rare spinocalanid copepods from the eastern North Atlantic, with descriptions of new species of the genera Spinocalanus and Teneriforma (Copepoda: Calanoida). *Mitteilungen aus dem Hamburgischen Zoologischen Museum und Institut* **86:** 185–208.

Shimode S, Toda T, Kikuchi T. 2000. *Ryocalanus spinifrons*, a new species of Ryocalanidae (Copepoda: Calanoida), from the southwestern part of Sagami Bay, Japan. *Hydrobiologia* **432:** 127–133.

Stamatakis A. 2006. RAxML-VI-HPC: maximum likelihood-based phylogenetic analyses with thousands of taxa and mixed models. *Bioinformatics (Oxford, England)* **22:** 2688–2690.

Stamatakis A. 2014. RAxML version 8: a tool for phylogenetic analysis and post-analysis of large phylogenies. *Bioinformatics* **30:** 1312–1313. Available at: http://bioinformatics.oxfordjournals.org/content/early/2014/01/21/bioinformatics.btu033.abstract?keytype=ref&ijkey=VTEqgUJYCDcf0kP (accessed October 16, 2018).

Stocsits RR, Letsch H, Hertel J, Misof B, Stadler PF. 2009. Accurate and efficient reconstruction of deep phylogenies from structured RNAs. *Nucleic Acids Research* **37:** 6184–6193.

Tamura K, Stecher G, Peterson D, Filipski A, Kumar S. 2013. MEGA6: Molecular Evolutionary Genetics Analysis version 6.0. *Molecular Biology and Evolution* **30:** 2725–2729.

Tanaka O. 1956. Rare species of Copepoda Calanoida taken from the Izu region. *Breviora* **64:** 1–8.

Thum RA, Harrison RG. 2008. Deep genetic divergences among morphologically similar and parapatric *Skistodiaptomus* (Copepoda: Calanoida: Diaptomidae) challenge the hypothesis of Pleistocene speciation. *Biological Journal of the Linnean Society* **96:** 150–165.

White TJ, Bruns T, Lee S, Taylor J. 1990. Amplification and direct sequencing of fungal ribosomal RNA genes for phylogenetics. In: Innis MA, Gelfand DH, Sninsky JJ, eds. *PCR protocols*. New York: Academic Press, 315–322.